Atmos. Chem. Phys. Discuss., doi:10.5194/acp-2016-925, 2016
Manuscript under review for journal Atmos. Chem. Phys.
Published: 10 November 2016

Atmospheric Chemistry and Physics Discussions

PHENOMENOLOGY OF HIGH OZONE EPISODES IN NE SPAIN

Xavier QUEROL[1], Gotzon GANGOITI [2], Enrique MANTILLA[3], Andrés ALASTUEY[1], Maria Cruz MINGUILLÓN[1], Fulvio AMATO[1], Cristina RECHE[1], Mar VIANA[1], Teresa MORENO[1], Angeliki KARANASIOU[1], Ioar RIVAS[1], Noemí PÉREZ[1], Anna RIPOLL[1], Mariola BRINES[1], Marina EALO[1], Marco PANDOLFI[1], Hong-Ku LEE[4], Hee-Ram EUN[4], Yong-Hee PARK[4], Miguel ESCUDERO[5], David BEDDOWS[6], Roy M. HARRISON[6+], Amelie BERTRAND[7], Nicolas MARCHAND[7], Andrei LYASOTA[8],Bernat CODINA[8], Miriam OLID[8], Mireia UDINA[7], Bernat JIMÉNEZ B.[8], Rosa M. SOLER[8], Lucio ALONSO[2], Millán MILLÁN [3],Kang-Ho Ahn[4]

[1] Institute of Environmental Assessment and Water Research, IDAEA-CSIC, C/ Jordi Girona 18-26, 08034 Barcelona, Spain
[2] Escuela Técnica Superior Ingeniería de Bilbao, Departamento Ingeniería Química y del Medio Ambiente, Universidad del País Vasco UPV/EHU, Urkixo Zumarkalea, S/N, 48013 Bilbao, Spain
[3] Centro de Estudios Ambientales del Mediterráneo, CEAM, Unidad Asociada al CSIC, Parque Tecnológico C/ Charles R. Darwin, 14 46980 Paterna, Valencia, Spain
[4] Department of Mechanical Engineering, Hanyang University, Ansan 425-791, Republic of Korea
[5] Centro Universitario de la Defensa de Zaragoza, Academia General Militar, Ctra. de Huesca s/n, 50090 Zaragoza, Spain
[6] Division of Environmental Health & Risk Management. School of Geography, Earth & Environmental Sciences. University of Birmingham. Edgbaston, Birmingham B15 2TT, UK
[7] Aix Marseille Université, CNRS, LCE UMR 7376, 13331 Marseille, France
[8] Department of Astronomy and Meteorology, Faculty of Physics, University of Barcelona, Martí I Franquès 1, 08028 Barcelona, Spain

[+]Also at: Department of Environmental Sciences/Center for Excellence in Evironmental Studies, King Abdulaziz University, Jeddah, Saudi Arabia.

ABSTRACT

Ground level and vertical measurements (coupled with modelling) of ozone (O_3), other gaseous pollutants (NO, NO_2, CO, SO_2) and aerosols were carried out in the plains (Vic Plain) and valleys of the northern region of the Barcelona Metropolitan Area (BMA) in July 2015; an area typically recording the highest O_3 episodes in Spain. Our results suggest that these very high O_3 episodes were originated by three main contributions: (i) the surface fumigation from high O_3 reservoir layers located at 1500-3000 m a.g.l., and originated during the previous day(s) injections of polluted air masses at high altitude; (ii) local/regional photochemical production and transport (at lower heights) from the BMA and the surrounding coastal settlements, into the inland valleys; and (iii) external (to the study area) contributions of both O_3 and precursors. These processes gave rise to maximal O_3 levels in the inland plains and valleys northwards from the BMA when compared to the higher mountain sites. Thus, a maximum O_3 concentration was observed within the lower tropospheric layer, characterised by an upward increase of O_3 and black carbon (BC) up to around 100-200 m a.g.l. (reaching up to 300 µg/m^3 of O_3 as a 10-s average), followed by a decrease of both pollutants at higher altitudes, where BC and O_3 concentrations alternate in layers with parallel variations, probably as a consequence of the atmospheric transport from the BMA and the return flows (to the sea) of strata injected at certain heights the previous day(s). At the highest altitudes reached in this study (900-1000 m a.g.l.) during the campaign, BC and O_3 were often anti-correlated or unrelated, possibly due to a prevailing regional/hemispheric contribution of O_3 at those altitudes. In the central hours of the days a homogeneous O_3 distribution was evidenced for the lowest 1km of the atmosphere, although probably important variations could be expected at higher levels, where the high O_3 return strata are injected according to the modelling results and free sounding data.

Atmos. Chem. Phys. Discuss., doi:10.5194/acp-2016-925, 2016
Manuscript under review for journal Atmos. Chem. Phys.
Published: 10 November 2016

Atmospheric Chemistry and Physics Discussions

Relatively low concentrations of ultrafine particles (UFP) were recorded in the 100-200 m a.g.l. atmospheric layer where concentrations of O_3 were high; and nucleation episodes were only detected into the boundary layer.

Two types of O_3 episodes were identified: Type A) with major exceedances of the O_3 information threshold (180 µg/m^3 on an hourly basis) caused by a clear daily concatenation of local/regional production with accumulation (at upper levels), fumigation and direct transport from the BMA (closed circulation); and Type B) with regional O_3 production without major recirculation (neither fumigation) of the polluted BMA/regional air masses (open circulation), and relatively lower O_3 levels.

The interpretation of O_X (O_3+NO_2) experimental data from strategically selected monitoring sites on the coast and inland, together with the photochemical modelling results have allowed to study the O_3 phenomenology associated with the onset and development of severe episodes in the region of Catalonia in NE Spain.

To implement potential O_3 control and abatement strategies two major key tasks are proposed: (i) meteorological forecasting, from June to August, to predict recirculation episodes so that NO_X and VOCs abatement measures can be applied before these episodes start; (ii) sensitivity analysis with high resolution modelling to evaluate the effectiveness of these potential abatement measures of precursors for O_3 reduction.

Keywords: O_3, photochemistry, air pollution, air quality, NO_x

INTRODUCTION

Ozone (O_3) is an airborne secondary pollutant that is produced through the photo oxidation of volatile organic compounds (VOCs) in the presence of nitrogen oxides (NO_X=NO+NO_2), with more intensive production in high insolation regions. It is well known that its formation processes are very complex and that the reaction and production rates are not linear (Monks et al., 2015 and references therein). According to EEA (2015) 97% of the European population is exposed to O_3 concentrations that exceed the WHO guideline (see below) for the protection of the human health. The complexity of this pollutant is also reflected in its air quality targets; thus, the European air quality directive 2008/50/EC establishes a number of O_3 target values (which are not legally binding, as opposed to the limit values set for the majority of pollutants):

- A human health target value fixed at 120 µg/m^3 as 8 hours maxima in a day that should not be exceeded in more than 25 days/year as a three-year mean. This target value was (arbitrarily) increased from the recommended 100 µg/m^3 in the WHO air quality guidelines (where no exceedances are recommended).
- A population information hourly threshold of 180 µg/m^3.
- A population alert hourly threshold of 240 µg/m^3.
- A vegetation protection target, AOT40 [expressed in µg/m^3·h], as the sum of the excess of hourly concentrations above 80 µg/m^3 along a given period using only hourly values measured between 8:00 and 20:00 h, Central Europe Time (CET), for every day. Hourly AOT40 from May to July should not exceed 18.000 µg/m^3·h O_3 as a mean for 5 years.

NO_x has a catalytic effect in O_3 generation, and is only removed from the system by either deposition or oxidation to nitric acid (HNO_3) and reaction with VOCs to yield secondary aerosols. Consequently, O_3 generation involves not only local and regional air masses but also long-range

Atmos. Chem. Phys. Discuss., doi:10.5194/acp-2016-925, 2016
Manuscript under review for journal Atmos. Chem. Phys.
Published: 10 November 2016

Atmospheric Chemistry and Physics Discussions

transport. Thus, as a general observation, long range transport of O_3 and its precursors influence markedly the background O_3 levels in Europe (UNECE, 2010; Doherty et al., 2013). However, this situation might be very different when considering the high summer O_3 episodes of Southern Europe (e.g. Millán et al., 1997, 2000; Palacios et al., 2002; Castell et al., 2008a, 2008b, 2012; Stein et al., 2005; Escudero et al., 2014; Pay et al., 2014; Querol et al., 2016).

In the Western Mediterranean basin the problem of tropospheric O_3 has been intensively studied since the early 1980s (Millán et al., 1991, 1996a, 1996b, 1996c, 2000, 2002; Millán, 2002a; Millán and Sanz, 1999; Mantilla et al., 1997; Salvador et al., 1997, 1999; Gangoiti et al., 2001; Stein et al., 2004, 2005; Doval et al., 2012; Castell et al., 2008a, 2008b, 2012; Escudero et al., 2014). Results have evidenced that (i) the meteorology driving O_3 fluctuation in this region is markedly influenced by a very complex orography with high mountain chains surrounding the basin; (ii) in summer, the lack of a marked synoptic advection caused by the presence of the Azores anticyclone and the Iberian and north African thermal lows, together with the sea and land breezes, give rise to air mass recirculation episodes (lasting for several days); and (iii) during these summer vertical and horizontal recirculations of air masses loaded with O_3 precursors and coinciding with high insolation and elevated biogenic VOCs (BVOCs) emissions (Seco et al., 2011), high O_3 concentrations may be recorded.

Millán's team results demonstrated that Western Mediterranean basin dynamics are very different from those in Central Europe. The latter are dominated by neutral-cloudy conditions, where O_3 episodes are usually associated with advection, and transformation takes place within large displacements of air masses. In days, morning fumigation from a high O_3 residual (and stratified) boundary layer (BL) formed over the previous days, in addition to local formation in the sunny midday period may give rise to peak O_3 episodes if conditions persist after several days. In contrast, vertical re-circulations developed over all Western Mediterranean coastal areas, determine a very different O_3 dynamics. Air masses travel all the way from the sea to the continental divide, or to the top of the Apennines in the case of Italy. These air mass circulations create layers over the sea at various altitudes, with accumulated pollutants/precursors in several stages of transformation. These processes can occur during a few consecutive days (e.g. 10 days, Millán et al., 1997). The layers already over the basin descend from 1000-1500 m a.s.l. during the day and can reach the lower levels, providing a high background O_3 to coastal cities when the sea and up-slope breezes build up (Millán et al., 2000). Layers, by definition, are stratified and decoupled from each other so they can move in different directions and speeds at their own heights.

Rodriguez et al. (2002) and Cusack et al. (2013) showed that these high background O_3 episodes are characterised also by high particulate matter (PM) concentrations, mostly due to the formation of secondary organic and inorganic aerosols. Such episodes are very common from June to August, and are usually limited by the occurrence of episodic Atlantic or African advective conditions that help (especially the first) to ventilate the Western Mediterranean basin. Minguillón et al. (2015) demonstrated also the occurrence of very intense aerosol nucleation episodes under high insolation scenarios in the vertical column (from 200 to 1000 m.a.s.l.) over the city of Barcelona. As the surface air ascends, aerosols are diluted and levels of O_3 are expected to increase.

The Barcelona Metropolitan Area (BMA) is a highly industrialised and dense urban agglomeration extending over the Mediterranean side of northeast Spain. High anthropogenic NO_X emissions arise both from road (and shipping) traffic and power generation, which combined with BVOCs emissions, very often cause severe O_3 episodes in the northern plains and valleys (Toll and

Atmos. Chem. Phys. Discuss., doi:10.5194/acp-2016-925, 2016
Manuscript under review for journal Atmos. Chem. Phys.
Published: 10 November 2016

Atmospheric Chemistry and Physics Discussions

Baldasano, 2000; Barros et al., 2003; Gonçalves et al., 2009; Valverde et al., 2016; Querol et al., 2016). The urban plume is transported inland by sea breezes, heading North channelled by N-S valleys that cross the coastal and pre-coastal Catalan Ranges to an intra-mountain plain (the Vic Plain) where the cities of Manlleu, Vic and Tona lie, 40-65 km north of Barcelona (Figure 1). A mean of 15 annual exceedances of the hourly O_3 information threshold/site are recorded at the urban background monitoring sites of these cities (Querol et al., 2016). In 2015, 96 out of the 115 hours exceeding the O_3 information threshold in the whole Catalonia air quality monitoring network were recorded in the area within 40-90 km north of Barcelona (towards the Pyrenees), and 82 in the Vic Plain itself (http://www.gencat.cat/mediamb/qaire/ciozo.htm).

This work focuses on an intensive campaign on O_3 and particulate pollutants performed in and around the BMA during July 2015, when high O_3 episodes were recorded, with the aim of investigating the origin of the most intense O_3 events in north-eastern Spain. To this end, regional air quality monitoring network data, passive dosimeters at ground level, vertical profile measurements of O_3 and ultrafine particles (UFP) in the Vic Plain, and modelling tools were employed.

METHODOLOGY

Study area

This study is set in central Catalonia (Figure 1), in north-eastern Spain. The mountain ranges surrounding the area (Pyrenees and Catalan Coastal Ranges) protect the area from the advection of Atlantic and continental air masses but hamper dispersion of pollutants. The typical winds in the region are the Tramontana (northern winds), the Mistral or Cierzo (north-western winds channelled by the Ebro valley) and the sea breezes in the coastal region. In summer, daytime up-slope winds combined with sea breezes may result in air masses penetrating 120-160 km inland that are injected aloft the top of the mountains, and follow the return night flows towards the sea (Millán, 2014). This scenario of air mass regional recirculation during periods of several days prevails in summer (Millán et al., 1997 and 2000). Hence, summer pollution events are characterised by (i) the absence of large-scale forcing and the predominance of mesoscale circulations; (ii) the formation of a thermal low at a peninsular level (forcing the convergence of surface winds from the coastal areas towards the central plateau with strong levels of subsidence over the Western Mediterranean basin); and (iii) combined breeze dynamics, resulting in the recirculation and accumulation of pollutants over the whole Western Mediterranean basin, including the Eastern Iberian peninsula (Millán 2014 and Millán et al., 1997, 2000).

The region is characterised by important atmospheric pollutant emissions from road traffic, industries, biomass burning, livestock, and airport and shipping activities, which coupled with high solar radiation turns into a high rate of secondary PM and O_3 formation (Rodriguez et al., 2002). Industrial activities are mostly concentrated in the Barcelona and Tarragona provinces, and include 19 combustion/energy plants, 84 metallurgy plants and 70 mineral industries. Road traffic, airport and shipping emissions are concentrated in the Barcelona area with >3.5 10^6 vehicles (0.6 per inhabitant, with high diesel and motorbike proportions; DGT, 2014), >45 10^6 tons of shipping transportation, and >37 10^6 aircraft passengers in 2014 (Ajuntament de Barcelona, 2015).

Agriculture, livestock and biomass burning emissions are spread over the rural areas but concentrated in the core study area, the Vic Plain: a 30 km long depression in the north-south

Atmos. Chem. Phys. Discuss., doi:10.5194/acp-2016-925, 2016
Manuscript under review for journal Atmos. Chem. Phys.
Published: 10 November 2016

Atmospheric Chemistry and Physics Discussions

direction located 60 km to the north of Barcelona. The area is surrounded by mountains is affected by thermal inversions during the night. The summer atmospheric dynamics dominated by sea breezes from the southern sector, channelled through the valleys formed by the coastal ranges, giving rise to the transport of pollutants from the BMA and the numerous surrounding highways.

Ground level measurements

Automatic measurements of gaseous pollutants

Measurements of gaseous pollutants were performed at 48 sites belonging to the regional air quality network (Figure 1, XVPCA; http://dtes.gencat.cat/icqa, Table S1) from 01 to 31/07/2015. Continuous measurements of O_3, NO, NO_2, CO and SO_2 were carried out using MCV 48AV UV photometry analysers, Thermo Scientific chemiluminescence analysers (42i-TL), Teledyne 300 EU Gas filter correlation analysers; and Teledyne 100 EU UV fluorescence analysers, respectively.

Measurements of gaseous pollutants with passive dosimeters

Diffusion tubes for NO_2 and O_3 sampling (Gradko Environmental) were deployed at 17 locations between the cities of Barcelona and Ripoll (Figure 1) covering strategic areas not monitored by the regional air quality network. The dosimeters were positioned along two main river basins in the study area (Besòs/Congost and Tordera), from the BMA to the Vic Plain. Sampling points were selected avoiding the direct influence of vehicular emissions and located at a height of approximately 2.5 m above ground level. One sample per site and sampling period (01-14 and 14-29/07/2015) were collected. After exposure, samples were stored at 4 °C until analysis.

Replicas were placed in 9 locations, showing good reproducibility of the results (relative errors of 5%±6% for O_3 and 4%±7% for NO_2). Dosimeters were collocated also at some XVPCA sites for comparison with reference measurements (6 samples for O_3 at Vic (VIC), Montcada (MON) and Montseny (MSY); and 10 samples for NO_2 at Santa María de Palau Tordera (SMPT), Palau Reial (PLR), Tona (TON), Manlleu (MAN), and Granollers (GRA)). Correction factors were obtained from the comparison between dosimeter and reference data (Dosimeter O_3 = 1.01*Reference O_3 + 17.43, R^2 = 0.97; and Dosimeter NO_2 = 1.27*Reference NO_2 + 1.14, R^2 = 0.90, in all cases in $\mu g/m^3$) and then applied to the dosimeter data (supplementary information Figure S1).

NH_3 passive samplers (CEH ALPHA, Tang et al., 2001) were also used in 30 specific points.

O_x concentrations

O_x values (NO_2+O_3) were calculated to complement the interpretation of O_3 concentrations. The concept of O_X was initially proposed by Kley and Geiss (1994) to analyse the O_3 spatial and time variability by diminishing the effect of titration of O_3 by NO ($NO+O_3 \rightarrow NO_2+O_2$, with the subsequent consumption of O_3) in highly polluted areas with high NO concentrations.

Laboratory van in Vic

A laboratory van was deployed next to the Vic air quality station during 10-17/07/2015. Eight-hour $PM_{2.5}$ samples were collected three times per day (00:00-08:00, 08:00-16:00, and 16:00-00:00 UTC) by means of Digitel DH80 high volume samplers (30 m^3/h) on Pallflex quartz fiber filters (QAT 150 UP). Filters were conditioned at 20-25°C and 50% relative humidity over at least 24 h before and after sampling to determine gravimetrically the $PM_{2.5}$ concentration. Subsequently a detailed chemical analysis following the procedure described by Querol et al. (2001) was carried out.

Atmos. Chem. Phys. Discuss., doi:10.5194/acp-2016-925, 2016
Manuscript under review for journal Atmos. Chem. Phys.
Published: 10 November 2016

Atmospheric Chemistry and Physics Discussions

Hourly equivalent Black Carbon (BC) in $PM_{2.5}$ concentrations were determined by a multi-angle absorption photometer (MAAP, model 5012, Thermo). PM_1, $PM_{2.5}$ and PM_{10} hourly concentrations were determined by an optical particle counter (GRIMM 1107).

Vertical profiles

During 14-17/07/2015 several vertical profiles up to 1550 m a.s.l. (1000 m a.g.l.) were performed by means of a tethered balloon (details can be found in Table S2) in the city of Vic (Figure 1), at less than 200 m from the laboratory van and the Vic air quality station. The tethered balloon of 27 m^3 filled with helium was equipped with an instrumentation pack attached 30 m below the balloon. This setting has been successfully used in previous studies (Minguillón et al., 2015), hence the lack of a fixed support for the instrumentation pack is not expected to hinder the quality of measurements.

The instruments included in the pack were:

- A miniaturized condensation particle counter (Hy-CPC) measuring particle number concentration larger than 3 nm with a time resolution of 1 s and a flow rate of 0.125 L/min, using isopropyl alcohol as the working fluid (Lee et al., 2014). The particle number concentration measured by the Hy-CPC will be referred to as N_3. Prior studies have demonstrated the agreement of the Hy-CPC and conventional TSI CPCs (Minguillón et al., 2015).
- A miniaturized nano-particle sizer for the determination of the particle number size distribution (Hy-SMPS, Figure S2) in the range 8-245 nm with a time resolution of 45 s and a flow rate of 0.125 L/min (Lee et al., 2015). The instrument output agreed well with the results from a Scanning Mobility Particle Sizer (SMPS), composed by a Differential Mobility Analyser (DMA, TSI 3081) coupled with a CPC (TSI 3772) (Figure S3, Hy-SMPS= 0. 71*Reference SMPS + 999, R^2 = 0.88). SPECIFY SIZE RANGES TO ACCOUNT FOR THIS LARGE DIFFERENCES
- A miniaturized optical particle counter (Hy-OPC, Figure S2) measuring particle number concentrations in the ranges 0.3-0.5 µm ($N_{03-0.5}$), 0.5-1.0 µm ($N_{0.5-1.0}$), 1.0-2.0 µm ($N_{1.0-2.0}$), and 2.0-5.0 µm ($N_{2.0-5.0}$), with a time resolution of 1 s and a flow rate of 1 L/min.
- A microaethalometer (MicroAeth AE51), which provided BC concentrations derived from absorption measurements on a 5 min basis with a flow rate of 0.15 L/min.
- A portable O_3 monitor that measures concentrations every 10 s based on UV absorption (POM^{TM} 2B Technologies, Figure S2). The personal POM O_3 monitor was compared with the O_3 concentrations from the nearby reference station, yielding good results (n=34 min data; POM O_3= 0.85* ReferenceO_3 +0.56, R^2 = 0.93) (Figure S1). The measured vertical O_3 concentrations reported in this study were normalized to standard temperature and pressure conditions (25 °C, 1013.2 hPa).
- A Global Position System (GPS).
- Temperature, relative humidity, pressure, wind direction and wind speed sensors.

Moreover, another sounding was carried out on the 16/07/2015 at 11:00 UTC. A free balloon was used with an instrumentation pack equipped with a Hy-CPC, a GPS, a temperature sensor, and a relative humidity sensor. The pack was placed in an insulated box (Figure S4).

Meteorological parameters

Atmos. Chem. Phys. Discuss., doi:10.5194/acp-2016-925, 2016
Manuscript under review for journal Atmos. Chem. Phys.
Published: 10 November 2016

Atmospheric Chemistry and Physics Discussions

30-minute meteorological data from 11 sites located throughout the study area in the proximity of air quality monitoring sites were provided by Meteocat (Meteorological Office of Catalonia) (Figure 1 and Table S3). Hourly average wind components were calculated and used in polar plots with hourly O_3 and O_X concentrations, by means of the OpenAir software (Carslaw, 2012). These are bivariate polar plots concentrations are shown to vary by wind speed and wind direction as a continuous surface.

Modelling system for O_3

The ambient O_3 concentrations were modelled using the ARAMIS (A Regional Air Quality Modelling Integrated System) high resolution modelling system that integrates the Weather Research and Forecasting model (WRF-ARW) version 3.1.1 (Skamarock et al., 2008) as a meteorological model, the High Resolution Emission Model (HIREM) (Soler et al., 2004, 2011 and 2015), and the Models-3 Community Multiscale Air Quality Modelling System (Models-3/CMAQ) (Byun and Ching, 1999) as a photochemical model. The modelling system was configured using four nested domains, D1, D2, D3, and D4 with horizontal grids of 27, 9, 3 and 1 km, respectively. Initial and boundary conditions for the meteorological model were taken for the European Centre for Medium-Range Weather Forecast global model (ECMWF) with a 0.5º x 0.5º resolution, and the boundary conditions are forced every 6 h, whilst for the photochemical model initial and boundary conditions model came from a vertical profile supplied by CMAQ itself. Domains are run in one-way nesting and 24 h spin-up was performed to minimize the effects of initial conditions for the inner domains. The output data is saved every hour. ARAMIS is continuously updated, it has been extensively evaluated (Soler et al., 2015) to simulate air quality over regional and local scales. In the present study the domain D3 was used, which covers the area of interest.

RESULTS AND DISCUSSION

Meteorological background and diurnal cycles of pollutants

Two types of episodes that will be discussed in the following sections were identified concerning the meteorological patterns and the O_3 concentrations recorded.

- Type A episode: Under “usual summer conditions”, with the Azores High located west of Iberia, and a ridge of high pressures extending into southern France, air masses in the Western Mediterranean basin rotate clockwise (anticyclonic) during the day, changing the direction at nighttime (Gangoiti et al., 2001), while the Atlantic gap winds (through the Ebro and Carcassonne valleys), weaken during daytime due to inland sea breezes and become strengthened during nighttime (Millán et al. 1997; Gangoiti et al., 2001, Gangoiti et al., 2006 and Millán 2014). In such conditions, the air layers over the sea in front of Barcelona tend to move within the south-westerlies during the day, following the clockwise rotation, i.e. towards Southern France and the Gulf of Genoa, and within the northerlies (towards Valencia) during the night. Thus, direct transport of O_3 and precursors from the Fos-Berre-Marseille-Piombino (Livorno) area towards the BMA is weak or null. However, indirect transport is more likely, first into the sea during nighttime conditions, and then following the daytime south-westerlies for the combined coastal sea-breeze and anticyclonic gyre at the coastal strip of Catalonia, which could bring a fraction of the referred O_3 and precursors originated in southern France, together with those emitted at the eastern coast of Iberia

Atmos. Chem. Phys. Discuss., doi:10.5194/acp-2016-925, 2016
Manuscript under review for journal Atmos. Chem. Phys.
Published: 10 November 2016

Atmospheric Chemistry and Physics Discussions

- Type B episode: When the anticyclone establishes over Central Europe with relative low pressures to the West over the Atlantic, the flow pattern over the Western Mediterranean changeS: southerly winds blow at height over eastern Iberia, while at ground level, gap winds may weaken or stop the Mistral and the Tramontana winds in the Gulf of Lion, and Barcelona could then be directly affected by O_3 and precursors, coming with the easterlies blowing at the marine boundary layer (emissions from Corsica, Sardinia and Italy). However, under these atmospheric conditions O_3 levels did not reach the observed values found during episodes type A, and the O_3 daily records did not show the classical pattern of accumulation from one day to the next, characteristic of the highest O_3 episodes in the Western Mediterranean (Millán et al., 1997, 2000 and Castell et al., 2008a)

Under the above "usual summer conditions", Millán et al. (1991, 1996a, b, c, 1997, 2000, 2002), Gangoiti et al., (2001), and Castell, (2008a) demonstrated the vertical recirculation of O_3-rich masses in the western Mediterranean, with O_3 being formed from precursors transported inland by the combined up-slope and sea breeze winds. O_3 loaded air masses, elevated by topography and sea-mountain breezes will be transported back to the coastal area at a certain altitude during the day and accumulates in elevated stably stratified layers at the coastal areas during the late evening and night. During nighttime and at ground level O_3 depletion dominates mainly in urban and industrial centers, driven by reaction with new emissions, which at the coastal area are transported offshore within the stable surface drainage flows.

The synoptic atmospheric situation in July 2015 was characterized by an intense high pressure system over central and southern Europe during almost the whole month (Figure S5). Type A and B scenarios alternated, transporting warm air masses from North Africa towards higher latitudes by the anticyclonic dynamic and reaching extremely high temperatures in Europe. The stagnation of air masses induced a regional meteorological scenario in the area under study, characterized by local/regional re-circulations and sea-land breezes, both channelled by the complex topography. The flow pattern, together with the observed stably stratified layers developed up to a height of 2000-2500 m a.s.l. (Figure S5) associated with subsidence, enhanced the accumulation of pollutants and caused several pollution episodes in the north-eastern Iberian Peninsula. Coastal and pre-coastal locations (Barcelona) were mainly affected by daily sea breezes, starting blowing from the east (around 08:00 UTC) and turning progressively to south and southwest. The sea breezes were channelled through the valleys, which are mainly located following a north-to-south axis, and arrived to the monitoring stations predominantly from a southerly direction. However, during the night atmospheric conditions were much more stable with flow patterns dominated by land breezes from N-NW.

The VIC site was characterised by stagnant conditions during the day, reaching the maximum wind speed (4 m/s on average) at around 15:00 UTC, when sea-breeze intensity was at the highest (Figure 2). During the night very light winds blew from the north (Figure 2). During the periods 14-20/07/2015 (episode type A) and 03-06/07/2016 (episode type B) the sea breeze blew from 10:00 to 18:00 and 10:00 to 21:00 UTC, respectively; but in the first one the wind speed was higher (maximum of 2.7 m/s as an average for the period) and maximal at 14:00 UTC, whereas in the second wind speed was lower, with a maximum mean value for the period of 2.4 m/s at 17:00 UTC, but only 1.5 m/s at midday.

Averaged ground O_3 concentrations during type A episode recorded at VIC were clearly influenced by these wind patterns, showing a typical midday peak, followed by a higher peak at 13:00-14:00 UTC probably caused by the transport of BMA air masses by the breeze (Figure 2). Mean O_3 levels during this A episode reached 195 µg/m^3 at 13:00 UTC. During type B episode averaged O_3 levels

Atmos. Chem. Phys. Discuss., doi:10.5194/acp-2016-925, 2016
Manuscript under review for journal Atmos. Chem. Phys.
Published: 10 November 2016

Atmospheric Chemistry and Physics Discussions

were also very high (142 µg/m^3 at 14:00 UTC) but clearly lower than during the A episode (Figure 2).

Intensive surface measurements were only available for 10-17/07/2015 (when the mobile laboratory was working at VIC). Average SO_2 levels for this period (included in the type A episode) showed a similar daily pattern to that of O_3 (Figure 2) pointing to a probable Hewson's-type I fumigation process (Hewson, 1964, Geiger et al., 1992) when midday convective flows that abate to the surface a SO_2 rich layer accumulated in the limit of the boundary layer. Ground level concentrations of BC, NO_2 and PM_x showed a similar daily pattern driven by stagnation and traffic rush hour, with maxima concentrations around 06:00 UTC (08:00 h local time, Figure 2). Finally, extremely high concentrations of NH_3 (this is one of the most intensive farming regions of Spain and mean values of the Vic Plain dosimeters reached 30 µg/m^3 NH_3 for 01-31/07/2015) followed the typical midday maximum due to evaporative emissions from fertilisers, but the rapid increase of the wind speed and dilution by the growth of the PBL thickness (see vertical profiles of temperature, aerosols and O_3 at VIC in following sections) probably account for a reduction of ground level NH_3 concentrations during the central hours of the day (Figure 2).

The varying diurnal and nocturnal air mass patterns in the Vic Plain are also shown by the $PM_{2.5}$ chemical composition. Figure S6 shows the 8-h concentration patterns of selected components during the week period of 10-17/07/2015, including several days (14 to 17/07/2016) of the type A episode defined above, affected by polluted air masses from the BMA.

In addition to the regionally transported O_3, concentrations of elemental carbon (EC) and traffic and industry-related metals (including Zn, Cu, Pb, Sn and Sb) were notably enhanced at the end of the week, and were attributed to local sources. This enhancement was most obvious during the 00:00-08:00 UTC period (Figure S6), under calm or northerly low wind (drainage slope winds) carrying metallic pollutants from the Cu-smelter located 13 km to the north of Vic, and leading to high Cu, Zn, Sn, W, Pb and Sb concentrations on the nights of 15 and 16/07/2015 (Figure S6). The increase in EC was related to local traffic emissions during the morning rush hour as deduced from the peaking MAAP BC concentrations during 05:00-08:00 UTC (07:00-10:00 h local time), up to 5 µg/m^3 hourly BC, when compared to 3 µg/m^3 recorded as maximum traffic rush hour concentrations in the preceding days (data not shown). In contrast, the rise of organic carbon (OC) concentrations observed during 08:00-16:00 UTC is attributed to the formation of secondary organic aerosols (SOA).

Sulphate concentrations did not show any trend, as expected from secondary inorganic components present in relatively homogeneous concentrations on a regional scale, whereas nitrate (and in a minor proportion ammonium) concentrations increased during the evening periods as a result of gas/particle partitioning (Figure S6). Interestingly, the stronger southerly winds during the daytime in the second part of the week (see below) appear to have brought polluted air from the BMA as signalled by slightly higher V concentrations (tracer of fuel oil combustion); but also the fumigation from high strata (polluted for air masses that were injected the previous day-s) might account for these SO_2 and V increases.

The concentrations of mineral matter and all its components (Al, Fe, Mg, Li, Ti, Rb, Sr, Ti, As) were constant during the week, with relatively higher concentrations in the 08:00-16:00 UTC samples (Figure S6), indicating a higher resuspension caused by stronger afternoon winds. The increment on the 15/07/2015 (08:00-16:00 UTC) was attributed to resuspension of local dust, given that the occurrence of African dust outbreaks was not observed during this period.

Atmos. Chem. Phys. Discuss., doi:10.5194/acp-2016-925, 2016
Manuscript under review for journal Atmos. Chem. Phys.
Published: 10 November 2016

Atmospheric Chemistry and Physics Discussions

The free sounding measurements carried out at 11:00 UTC on 16/07/2015 revealed stratified air masses up to 3000 m a.g.l. (Figure S7). The vertical profiles of potential temperature, water vapour and aerosol concentration distributions can be used for the identification of atmospheric layers presenting different properties: a lower layer up to about 1100 m a.g.l. characterised by a relative high aerosol concentration, well mixed and with a relative high and uniform water vapour content. A clear discontinuity between 1100 to 1500 m a.g.l limits the mentioned lower layer and a series of stably stratified layers up to a height of 3000 m a.g.l. This layering of pollutants is probably related to the development of regional and mesoscale convective cells driven by the combined upslope and sea breeze flows developed the day before (Millán et al., 1997).

O_3 and O_X episodes

Figure S8 shows the average O_3 and O_X ground level concentrations recorded in July 2015 in the study area at the XVPCA air quality monitoring network and with the passive dosimeters. O_X maximum concentrations were recorded at the Vic Plain area and in the coastal sites at the northeast of Barcelona. This is due to the high O_3 concentrations in Vic and to a higher proportion of primary NO_2 (emitted mainly from diesel engines, and not formed in the atmosphere from NO titration by O_3) in the coastal cities, respectively.

In July 2015, the O_3 hourly information threshold was exceeded a total of 74 times at the XVPCA stations of Catalonia, 57 taking place in the Vic Plain stations (TON, VIC and MAN), and 69 in the surrounding areas (pre-Pyrenees, High Llobregat river and Montseny).

Figure 3 shows hourly O_3 concentrations for the study period from selected monitoring sites. O_3 concentrations recorded at a coastal (Begur, BEG; blue, 200 m a.s.l.) and a remote inland western pre-Pyrenean site (MSC, light green, 1570 m a.s.l.) (Figure 3a) show relatively narrow diurnal variations and multiday episodes, with low or enhanced concentrations, according to meteorological fluctuations. O_3 variations at the coastal BEG are opposed to those at the inland MSC: As shown by the polar plots from Figure 4, relatively low O_3 concentrations (but still high in absolute terms) were recorded at the BEG coastal site (easternmost site in this figure) when the wind blows from the sea, whereas polluted air masses are transported towards the inland remote MSC (westernmost location in the figure) site under the same meteorological conditions. Conversely, when westerly winds blow, the inland remote MSC site received relatively clean air masses with low O_3 (Figure 4), which are progressively loaded with regional pollution as these are transported towards the coastal BEG site.

Data from two urban background sites of Barcelona (PLR and CTL, 81 and 5 m a.s.l., grey and black in Figure 3b) show evidence of a high nocturnal O_3 consumption, with differences due to local NO_x traffic emissions. Following the transport of air masses by combined breezes, the two sites located in the northern periphery of the BMA, along the Besòs river valley (GRA and MON, 140 and 33 m a.s.l., orange and yellow in Figure 3c; 20 and 6 km from BMA in NE an NNE directions, respectively) show local O_3 production, with higher midday concentrations, while very low nocturnal levels reflect again the intensive O_3 consumption (in a densely populated basin). O_3 concentrations were closer between GRA and MON than between the two Barcelona urban sites (PLR and CTL).

Relevant O_3 net production and fumigation can be readily seen in the inner Vic Plain (TON, VIC and MAN; 620, 498, 460 m a.s.l.; red, pink and violet in Figure 3d; 45, 55 and 62 km from BMA in a NNE direction, respectively) as well as at the remote eastern pre-Pyrenean site of Pardines (PAR, brown, 1226 m a.s.l, 102 km from BMA in a NNE direction), where O_3 formation and fumigation seems to have already reached its maximum, and similar O_3 concentrations were recorded at all

Atmos. Chem. Phys. Discuss., doi:10.5194/acp-2016-925, 2016
Manuscript under review for journal Atmos. Chem. Phys.
Published: 10 November 2016

Atmospheric Chemistry and Physics Discussions

445 sites during the midday increase. This suggests that the intensity of O_3 formation and fumigation
446 was clearly reduced in the Vic Plain-Pyrenees transect with respect to the Barcelona-Vic Plain (an
447 intermediate production place would be MSY (720 m a.s.l.; green in Figure 5, 39 km from BMA in a
448 NE direction). Polar plots of GRA, TON, MSY, VIC, MAN show clearly that the highest O_3 levels were
449 recorded with wind blowing from the Direction where BMA is located (Figure 4).

450 As it can be observed in Figures 3 and 5, during two periods (01-02 and 07-20/07/2015) O_3
451 concentrations increased progressively from the Barcelona city towards the northern BMA (GRA
452 and MON), the intermediate MSY regional background area and towards the northern Vic Plain
453 sites; and from there it slightly decreased towards the eastern pre-Pyrenees (PAR) following the
454 midday-afternoon combined breeze transport (Figures 3 and 5). During these days, no exceedance
455 of the information threshold was produced in the urban environment; only sporadic
456 measurements above the human protection target value were recorded in the close surroundings
457 of Barcelona. However, frequent exceedances of both thresholds were recorded in a regional
458 transport context towards the north of the BMA.

459 While differences in O_3 concentrations between TON, GRA, MSY, BEG and CTL were observed
460 during the period 03-06/07/2015 (B type episode), O_X concentrations show a very similar behavior
461 along the Vic Plain, both qualitative and quantitative (Figure 5, O_X is not reported at BEG due to
462 the lack of NO_2 measurements). Conversely, in the period 07-20/07/2015 (that includes the A type
463 episode), characterized by a change in the synoptic conditions, differences in daily maximum O_X
464 values resemble the same behavior of O_3 alone, with a positive and marked inland gradient. O_3
465 concentrations at BEG, a coastal site far in the northeast were higher during the former period and
466 showed low intra-day variation, indicating a probable long range transport of polluted air masses
467 (Figure 5).

468 O_3 and O_X concentrations at the regional background site (MSY, 720 m a.s.l., green in Figure 5)
469 depict also the meteorologically influenced patterns but with a clear overlapped and pronounced
470 daily fluctuation, with marked higher concentrations indicating O_3 generation from a regional
471 origin, especially on 01-02 and 07-20/07/2015 (Figure 5).

472 Diurnal O_3 concentrations in the Vic Plain (around 460-620 m a.s.l.) were markedly higher than at
473 the coastal (CTL, PLR) sites, and slightly higher than at mountain sites (MSY, PAR and MSC, from
474 720, 1226 and 1570 m a.s.l.) during the 01-02 and 07-20/07/2015 periods. The O_3 hourly
475 information threshold of 180 $\mu g/m^3$ was exceeded 55 times in the Vic Plain (3 sites), with 50 of
476 these exceedances taking place during 01/07/2015 and 14-20/07/2015. For these exceedances, an
477 hourly contribution of up to 150 $\mu g/m^3$ of O_X (mostly O_3) both from fumigation of recirculated
478 return layers (injected at an altitude of 1500-3000 m a.g.l. in the prior day(s)), and from transport
479 and photochemical generation of O_3 of the BMA plume, might be estimated based on the
480 differences of the O_X early afternoon maxima recorded at the coastal BMA sites and the ones in
481 the Vic Plain.

482

483 Type A episode (14-20/07/2015)

484 During this episode, a progressive time shift of the daily hourly O_3 and O_X maxima was observed
485 from the Barcelona area (10:00 UTC, at CTL into the BMA) towards the metropolitan periphery
486 (11:00, at GRA), the intermediate mountain sites (13:00, MSY, 39 km from BMA), the Vic Plain
487 (12:00, 13:00 and 14:00, TON, VIC and MAN, 45, 55 and 62 km from the BMA, respectively) and
488 the northern pre-Pyrenean site (16:00, PAR, 102 km from BMA) (Figure 6). This variation points to
489 the process of O_3 and O_X formation with a mean O_X difference between the urban-coastal sites and

Atmos. Chem. Phys. Discuss., doi:10.5194/acp-2016-925, 2016
Manuscript under review for journal Atmos. Chem. Phys.
Published: 10 November 2016

Atmospheric Chemistry and Physics Discussions

the Vic Plain hourly maxima of around 115 µg/m^3 for the TON site, with a maximum average O_3 hourly levels of around 200 µg/m^3. These O_X differences are mostly due to O_3 differences (Figure 6). Accordingly, during these intense O_3 pollution episodes, more than 50% of the O_3 hourly maxima concentrations are attributable to (i) O_3 contributions from the previously referred surface fumigation of recirculated strata (over the VIC-MAN-TON area) containing the polluted air masses injected the day before by complex topographic induced circulations; and to (ii) the local O_3 generation and surface transport of the BMA plume into inland valleys. Attributing these O_3 exceedances to local/regional causes is also supported by the spatial distribution of the hourly O_3 maxima, the number of hourly exceedances of the information threshold, the time shift of the exceedances at the different sites (as moving towards the north) (Figure 7), and the polar plots of hourly O_3 concentrations pointing towards the BMA as main source region (Figure 4).

Thus during the A episode, O_3 has mostly a major local/regional origin (with O_X maximum hourly levels progressively increasing from 166 to 246 µg/m^3 from the BMA to the Vic Plain). The concatenation of daily cycles of regional/long range recirculation of air masses and regional/local O_3 production in the A episode accounted for the accumulation of O_X and the consequent exceedance of the hourly information threshold. Castell et al. (2008a) have already reported a correlation between their 'recirculation factor' (a meteorological parameter devised to increase with the concatenation of days with regional vertical recirculation of air masses) with the occurrence of O_3 episodes in 2003. The relevance of these recirculations in originating these high O_3 episodes in Southern Europe was highlighted already, not only by scientific papers by the CEAM's team but also assumed by the European Commission (EC, 2004).

Figures 8 and 9 show results the vertical profiles (0-1100 m a.g.l.) of O_3 concentrations, particle number concentrations for particles > 3 nm (red), 0.3-0.5 µm (blue), 0.5-1.0 µm (brown), ambient temperature, relative humidity and wind direction, obtained at the beginning of the A type episode (from 14 to 17/07/2015).

In the profiles from 07:06 to 08:21 UTC on the 14/07/2015, a boundary layer (150 to 250 m thick) with relatively high levels of N_3 (0.8 to 2.0 10^4 #/cm^3) was differentiated from the free troposphere (0.2 to 0.8 10^4 #/cm^3) (Figure 8). However, in the profile obtained from 09:42 to 10:52 UTC on 17/07/2015, the growth by convective turbulence accounts for a homogeneous boundary layer and profile of $N_{0.3\text{-}0.5}$ below 1000 m a.g.l. (Figure 8). Inside the boundary layer nucleation occurred (yellow to red areas in Figure 10 for 16/07/2015) regionally driven by photochemical processes. Minguillón et al. (2015) showed the occurrence of these nucleation events into the mixing layer as convective transport elevates and dilutes air masses from polluted areas under high insolation in Barcelona. During 14-16/07/2015 nucleation episodes occurred occasionally, but only inside the boundary layer. On the 17/07/2015 at 9:42-10:52 UTC new particle formation occurred probably at relatively high altitudes, also inside the boundary layer, as deduced from the high N_3 levels measured from 400 to 1000 m a.g.l., with concentrations reaching 1 10^4 #/cm^3, while simultaneously low concentrations (< 0.3 10^4 #/cm^3) were measured at ground level (Figure 8). This vertical gradient is not observed for the coarser particles ($N_{0.3\text{-}0.5}$ and $N_{0.5\text{-}1}$) and O_3 (Figures 8 and 9, for which relatively constant levels were measured inside the boundary layer), suggesting new particle formation.

On 14/07/2015 07:06-08:21 UTC a well stratified atmosphere (Figure9) with both thermal and O_3 layers is observed, with a general upward increasing trend for O_3 from 40 µg/m^3 at ground level to 150 µg/m^3 at 1000 m a.g.l. reflecting the effect of surface depletion by NO titration and by deposition during the night (Figure 9). From 13:49 to 15:03 UTC on the 14/07/2015 (Figure 9) the vertical profile changed substantially, with an already unstable atmosphere near the ground,

showing very high surface O_3 concentrations of 217 µg/m^3 that increase up to 330 µg/m^3 in a layer around 100 m a.g.l., decreasing again through an upper layer with values of 240 µg/m^3 until 300 m a.g.l. (where measurements were not available due to instrumental problems). This 100-200 m a.g.l. very high O_3 layer agrees with the modelled O_3 concentrations for the study area (Toll and Baldasano, 2000; Barros et al., 2003; Gonçalves et al., 2009) and reflects elevated O_3 concentrations due to local production and transport of O_3, that decrease from 100 m a.g.l. to the surface due to its titration, consumption and deposition. On 15 and 16/07/2015, a similar upward increasing O_3 gradient was observed in the early morning (Figure 10). On 17/07/2015 7:39-08:40 UTC O_3 concentrations were relatively constant, but showing also a strongly stratified profile, in the range of 100-165 µg/m^3 in the lower 500 m. In the last profile from 09:42 to 10:52 UTC, O_3 concentrations increased from 140 to 200 µg/m^3 from 200 to 1000 m a.g.l., but again a maximum close to 200 µg/m^3 was observed at the same height around 100 m a.g.l. (Figure 9).

Thus, vertical profiles of the type A episode are characterised in the early morning by a strong stratification, showing low ground level O_3 concentrations, due to low production (low insolation) and/or consumption (titration and deposition), and increasing concentrations with altitude. This variation is related to prevailing meteorological conditions enhancing local recirculation or larger scale transport with high O_3 masses injected (the day before) at certain altitudes by vertical recirculations into the residual layer, above the nocturnal surface stably stratified boundary layer. Nevertheless, during specific days, homogeneous O_3 vertical profiles up to 1000 m a.g.l. (the maximum height reached with captive sounding) were also evidenced, but probably not maintained at higher levels (where we were not able to measure with our system). Thus, as shown by the 4500 m profile measured with the free sounding on 16/07/2016 (Figure S7), high PM (and probably O_3) strata are present between 1500 and 3000 m a.g.l., these being probably the polluted air mases injected the day before in the northern mountain ranges and recirculated to the coast at certain altitudes (see modelling outputs below). On the other hand, with constant southerly winds (from the coastal area to the Vic Plain) usually associated with the combined sea-breeze and up-slope flows, O_3 was enriched in the lower 100-200 m atmospheric layer, generated by the intensive local photochemical production. O_3 concentrations reached maximal values (up to 330 µg/m^3) on the top of this layer, while they decreased at lower heights by titration and deposition, although hourly levels of 225 µg/m^3 were still recorded. These results are consistent with the gradient of O_3 concentrations between the Vic Plain (around 500 m a.s.l.) and the MSY mountain site (720 m a.s.l., and more close to the sea) during the episodes, (Figures 5 to 7). At higher altitude, O_3 concentrations decreased but were still high (150-240 µg/m^3) due to the O_3 formation in air masses constantly transported from the coastal area, which also incorporates O_3 and precursors recirculated the day before, as it is shown next.

Interesting results are also obtained by comparing the vertical profiles of BC and O_3 (Figure 11). BC is a tracer of local primary pollution at ground level, and of the potential transport and stratification of regional/local primary pollutants (together or not with regional O_3) when present at high altitude. On 14/07/2015 07:06-08:21 UTC, at 350 m a.g.l. (and similarly on 15-17/07/2015 but at varying heights, 100-350 m a.g.l.) a clear discontinuity is evidenced with sudden and simultaneous decreases of BC and O_3 above these heights. The relatively high BC levels within the lower layer suggest the nocturnal accumulation, while O_3 appears in strata (with low values near the ground due to titration and deposition) and with a high concentration just above that level (350 m), now with low BC concentrations. There is a further upward decrease of BC and an increase of O_3 up to the limit o the sounding (870 m).

The occurrence of an O_3 maximum layer around 100-200 m a.g.l., on top of the nocturnal stably stratified boundary layer reinforces the idea of an important local production contributing to an

Atmos. Chem. Phys. Discuss., doi:10.5194/acp-2016-925, 2016
Manuscript under review for journal Atmos. Chem. Phys.
Published: 10 November 2016

Atmospheric Chemistry and Physics Discussions

upward increase of O_3 inside the layer. Finally, at the highest altitudes reached in this study (900-1000 m a.g.l.), BC and O_3 concentrations were often anti-correlated or unrelated, possibly more related with aged air masses re-circulated within the whole region and with a mixed origin: including local-to-regional sources and more distant over the W-Mediterranean.

Figure 12 shows mean O_3 hourly concentrations recorded at VIC for the episodes A and B, as well as mean wind speed and directions. Mean hourly concentrations are characterized by an increase until 10:00-11.00 UTC, followed by an inflexion point and a more marked increase, with a maxima between 13:00 and 14:00 h UTC, and then a progressive decrease, more marked in the episode. As stated above, processes contributing to increase levels were attributable (ordered by importance) to fumigation, photochemical production and transport of high O_3 air masses, all controlled by insolation. Millán et al. (2000) described this characteristic diurnal O_3 pattern typically for inland valley stations (as in our case around 75 km from the coast), where the first O_3 increase is attributed to O_3 contributions from surface fumigation of high recirculated return strata as well as from the arrival of higher O_3 air masses transported by sea-breeze and the local photochemical production from precursors. On the other hand, the second O_3 concentration 'hump' is coincident with maximum wind speed and probably corresponds to a more intensified sea breeze transport compared with local photochemical formation and fumigation. Figure 12 shows that the two O_3 increases (and consequently the contributions from the 3 above processes) are more pronounced in the type A compared to the type B episode, and that the second maxima (more associated to inland surface transport by sea breeze) is wider, coinciding with a shift of the maxima wind speed towards the late afternoon, in the B episode.

Modelling outputs for the A episode points to light winds from the south, transporting pollutants from the BMA towards northern areas (including the Vic Plain), and triggering the hourly O_3 exceedances under the effect of the sea and land breeze transport. Thus, Figures 13 and 14 show the horizontal wind vector at 10 m a.g.l. and NO_2 and O_3 concentrations both at ground level and at a height above the surface layer, at different hours for two representative days of the type A and B episodes, respectively. During the type A episode day (15/07/2015), the effect of the land breeze transport accumulates NO_2 over the sea during the night, starting intense O_3 production when sun rises and sea breezes start the inland transport. Maximum concentrations of O_3, exceeding 180 $\mu g/m^3$ were calculated by the model and measured at the stations located in the Vic Plain (TON, VIC and MAN, Figure 14), although the model overestimated maximum O_3 concentrations in TON and VIC and delayed the hourly maximum value in all stations. The vertical distribution shows an important accumulation of around 110 $\mu g/m^3$ trapped in a reservoir layer at around 1500 m a.s.l. during the night (Figure 15), which will fumigate downwards into the new developing mixing layer during the following hours. Local O_3 production from fresh precursors accumulated during the night in the stably stratified surface layer and then progressed inland along the midday hours. This results in an O_3 enriched plume within a layer of 1000-1500 m depth in the late afternoon, following the model results (Figure 15). This mixing layer also incorporates O_3 from upper reservoir layers after fumigation during the inland travel. The O_3 located at upper levels can re-circulate back into the sea and it will be potentially available to be transported inland (Millán et al., 1997 and 2002), to re-start a new cycle the following day.

<u>Type B episode (03-06/07/2015)</u>

As opposed to episode A, during the type B episode and 22-31/07/2015, despite the high O_3 and O_X concentrations, these concentrations were very similar in the urban and remote coastal sites and all along the northern sites, including the Vic Plain. Hence, the averaged O_X hourly concentrations of all the study sites were close to those at the coastal urban site in Barcelona CTL

Atmos. Chem. Phys. Discuss., doi:10.5194/acp-2016-925, 2016
Manuscript under review for journal Atmos. Chem. Phys.
Published: 10 November 2016

Atmospheric Chemistry and Physics Discussions

(and in the case of the O_3 close to the remote coastal site of BEG) compared with the large differences reported for the A episode (Figure 6). The high O_X peak measured at the urban site during the mornings of the B period (Figure 6) and from 8:00 to 10:00 UTC in the average hourly patterns (Figure7) is due to the contribution of primary NO_2. According to Carslaw et al. (2016) the Euro 1 to Euro 2 diesel engines in Europe (early 1990s) emitted 5-10% of primary NO_2 and 90-95% of NO, whereas the Euro 4 to Euro 5 equivalent engines (2004 and 2009 onwards) emit 16-29% of primary NO_2 and 71-84% of NO.

Also as opposed to the A episode, during the B episode, O_X levels varied in a very narrow range from East (coastal) to West (mountains, MSC site) and from South (BMA) to North (Vic Plain) and at different heights (from Barcelona and BEG at sea level to MSC at 1570 m a.s.l.). Following the results of the model in the Figures 13 and 15, O_3 does not re-circulate around the region in this period. There is no accumulation from one day to the next in reservoir layers located over the region. Southerly winds blow at height during the whole period and the combined sea breeze and upslope winds developed at lower layers during daytime, after coupling with the southerlies, vent out the O_3 production and the rest of pollutants to the north. The circulation is open, as opposed to the type A episode, which show a closed circulation (it is never completely closed) (Millán et al., 1997, 2000). Unfortunately, vertical profiles of O_3, UFP, PM and BC profiles were not obtained for this episode.

Model outputs also evidence a net night and early morning transport of O_3 at lower layers from east and north-east during the B episode, supporting the hypothesis of a regional transport from Southern France, advecting aged air masses to the whole region, while O_3 and its precursors from the BMA were transported during the morning to the south-west regions (Figure 13) giving rise to hourly O_3 exceedances in some stations situated in this area. Figure 13 also shows that during this episode (03/07/2015) the combined sea-breeze and upslope wind transported O_3 and precursors to the western pre-Pyrenees area, and values lower than 180 $\mu g/m^3$ were measured and modelled in all monitoring stations and mainly in the Vic Plain. The vertical distribution of O_3 also shows relatively low concentrations over most of the domain (Figure 15).

CONCLUSIONS AND IMPLICATIONS FOR AIR QUALITY

Very high levels of O_3 were recorded in the plains and valleys of the northern regions surrounding the Barcelona Metropolitan Area (BMA) during July 2015, where 69 out of the 74 exceedances of the hourly O_3 information threshold measured in the entire air quality monitoring network of Catalonia were recorded. This represents a major environmental problem for which air quality managers must implement European and national legislation.

Both experimental measurements and modelling exercises suggest that these very intense O_3 episodes were originated by the concatenation of daily cycles of vertical recirculation of air masses that accumulated photochemically generated pollutants (Millán et al., 1997, 2000, 2002; Gangoiti et al., 2001 and Castell et al., 2008a, Valverde et al., 2016), favoured by the high BVOCs and anthropogenic NO_X emissions in the BMA region. The lower 1000 m a.g.l. were highly enriched in O_3 by fumigation from precursors and O_3 located at upper levels (1500-3000 m a.g.l). Additionally, local contributions of O_3 to these episodes were also demonstrated by soundings of the lower layers (0-1000 m a.g.l.). Thus, slightly higher concentrations of O_3 were measured in stations located at the plains and inland valleys than at higher altitudes (up to +30-40/$\mu g/m^3$ added to 180$\mu g/m^3$ reached in the mountain sites), due to the local photochemical production from fresh precursors emitted during the night and early morning, and their channelling within the combined

upslope and sea breeze circulation that transports O_3 and precursors from the BMA. Thus vertical profiles identified a high O_3 layer 100-200 m a.g.l., produced by these local processes and also by the high deposition and titration of O_3 at the lower 100m depth layer. In our (mostly rural) study low concentrations of ultrafine particles were recorded at this high O_3 100-200 m a.g.l. layer and nucleation episodes were only detected into the boundary layer, most of the days at the lower atmospheric levels.

Two types of high O_3 episodes (A and B) were identified in the area:

Type A episode: Characterized by major local/regional O_3 recirculation, fumigation, production and transport, superimposed on the typical regional/long range transport, and by the occurrence of major exceedances of the O_3 information threshold (14-20/07/2015). Surface fumigation from high O_3 return (to the sea) layers injected the day(s) before at altitudes of 1500-3000 ma.g.l., and recirculated over the VIC-TON-MAN area, as well as direct surface transport and formation of local/regional polluted air masses (with O_3 and precursors) from the BMA towards the north, decisively contributed to these exceedances. Thus, this atmospheric scenario is governed by poor ventilation under local breeze circulations and vertical recirculation of air masses over the study.

Type B episode: With a major regional transport O_3 contribution, yielding similar O_X levels at all monitoring sites of the study area, with the arrival of aged air masses from the east/northeast (high O_3 levels entering through the coast), but without major transport from BMA to the Vic Plain (3-6/07/2015), and without vertical recirculation of air masses over the study area. When sunlight activates atmospheric photochemistry in the early morning, the northern regions were loaded with air masses with lower content of O_3 precursors, since air masses were transported from the BMA to the southwest (parallel to the coast) from 00:00 to 09:00 h UTC. The combined breeze at midday favored the transport towards the northwest, rather than to the north, as described for the type A episode. In addition the aged air masses are not vertically recirculated and leave the region towards the north-east (to France). Thus, O_3 concentrations were still relatively high (exceeding 120 $\mu g/m^3$ but below 180 $\mu g/m^3$) due to local production from fresh precursors and background O_3 contributions from the western Mediterranean, but not enough to exceed the information threshold.

From the perspective of possible precursor abatement strategies, direct mitigation measures at the BMA would have had a minor effect on O_3 concentrations at the Vic Plain area during the type B episode. However, during the type A episode, a reduction of NO_x and/or VOCs emissions in the BMA, some days before and during the episode, might have an effect on O_3 concentrations recorded in the Vic Plain. Nonetheless, due to the non-linearity of the O_3 generation processes, sensitivity analysis with high resolution modelling is necessary to evaluate the possible effects in terms of absolute concentrations.

The use of O_X data from strategically selected monitoring sites in the east coast, western and central mountain areas, urban background sites of the BMA and sites in the Vic Plain, tracking the natural routes of pollutant transport, is a useful tool to assess the different regimes leading to high O_3 concentrations, and to differentiate between type A and type B episodes, with important implications in the design of potential abatement strategies.

To implement potential (and difficult) abatement strategies two major key tasks are proposed:

1. Meteorological forecast from June to August to predict recirculation episodes in order to apply abatement measures for O_3 precursors before a recirculation episode starts. As state

above, the relevance of these recirculations in originating these high O_3 episodes in Southern Europe was assumed already by the European Commission in 2004 (EC, 2004).

2. Sensitivity analysis with high resolution modelling to evaluate the effectiveness of NO_x and VOCs abatement measures on O_3 reduction.

ACKNOWLEDEGMENTS

The present work was supported by the Spanish Ministry of Economy and Competitiveness and FEDER funds under the project HOUSE (CGL2016-78594-R), by the Generalitat de Catalunya (AGAUR 2015 SGR33 and the DGQA). Part of this research was supported by the Korea Ministry of Environment through "The Eco-Innovation project". The participation of University of Marseille and University of Birmingham was partially supported by two TNA actions projects carried out under the ACTRIS2 project (grant agreement No. 654109) financed by the European Union's Horizon 2020 research and innovation program.. The support of the CUD of Zaragoza (project CUD 2013-18) is also acknowledged. We are very thankful to the Generalitat de Catalunya for supplying the air quality data from the XVPCA stations, to METEOCAT (the Meteorological Office of Catalonia) for providing meteorological data and to the IES J. Callís and the Meteorological Station from Vic for allowing the performance of the vertical profiles and mobile unit measurements, respectively.

REFERENCES

Ajuntament de Barcelona, 2015. Annual Statistics of the Barcelona City.http://www.bcn.cat/estadistica/catala/dades/anuari/cap15/index.htm

Barros N., Borrego C., Toll I., Soriano C., Jiménez P., Baldasano J.M., 2003. Urban Photochemical Pollution in the Iberian Peninsula: Lisbon and Barcelona Airsheds. J. Air & Waste Manage. Assoc. 53:347–359.

Byun D.W. and Ching J.K.S., 1999.Science algorithms of the EPA Models-3 Community Multiscale Air Quality (CMAQ) modeling system. National Exposure Research Laboratory, US Environmental Protection Agency, Research Triangle Park, NC: Atmospheric Modelling Division; 27711

Carslaw D.C., 2012. The openair manual – open-source tools for analysing air pollution data, Manual for version 0.7-0, King's College, London.

Carslaw D.C., Murrells T.P., Andersson J., Keenan M., 2016. Have vehicle emissions of primary NO2 peaked? Faraday Discussions, In press DOI: 10.1039/C5FD00162E

Castell N., Mantilla E., and Millán M.M., 2008a. Analysis of tropospheric ozone concentration on a Western Mediterranean site: Castellon (Spain). Environmental Monitoring and Assessment, 136, 3-11.

Castell N., Stein A.F., Salvador R., Mantilla E., and Millán M.M., 2008b.The impact of biogenic VOC emissions on photochemical ozone formation during a high ozone pollution episode in the Iberian Peninsula in the 2003 summer season. Advances in Science and Research, 2, 9-15.

759 Castell N., Tellez L., and Mantilla E., 2012. Daily, seasonal and monthly variations in ozone levels
760 recorded at the Turia river basin in Valencia (Eastern Spain). Environmental Science and
761 Pollution Research, 19, 3461-3480.
762 Cusack M., Pérez N., Pey J., Alastuey A. and Querol X., 2013. Source apportionment of fine PM and
763 sub-micron particle number concentrations at a regional background site in the western
764 Mediterranean: a 2.5 yr study. Atmos. Chem. Phys., 13, 5173-5187.
765 DGT, 2014.Dirección General de Tráfico: Anuario Estadístico General 2014.
766 http://www.dgt.es/es/seguridad-vial/estadisticas-e-indicadores/publicaciones/anuario-
767 estadistico-general/
768 Dieguez J.J., Millán M., Padilla L., Palau J.L., 2009. Estudio y evaluación de la contaminación
769 atmosférica por ozono troposférico en España. CEAM Report for the Ministry of Agriculture,
770 Food and Environment, INF FIN/O3/2009. 372 pp. http://www.magrama.gob.es/es/calidad-y-
771 evaluacion-ambiental/temas/atmosfera-y-calidad-del-aire/8_A_Informe_final_ozono-
772 ceam_Julio_2009_tcm7-152609.pdf
773 Dieguez J.J., Calatayud V., Mantilla E., 2014. CEAM Report for the Ministry of Agriculture, Food and
774 Environment, Fundación Biodiversidad. Informe Final. Memoria Técnica Proyecto CONOZE.
775 CONtaminación por OZono en España. 137 pp http://www.magrama.gob.es/es/calidad-y-
776 evaluacion-ambiental/temas/atmosfera-y-calidad-del-
777 aire/Informe_t%C3%A9cnico_CONOZE%5B1%5D_tcm7-330956.pdf
778 Doherty R.M., Wild O., Shindell D.T., Zeng G., Collins W.J., MacKenzie I.A., Fiore A.M., Stevenson,
779 D.S. Dentener, F.J., Schultz M.G., Hess P., Derwent R.G. and Keating T.J., 2013. Impacts of
780 climate change on surface ozone and intercontinental ozone pollution: A multi-model study.
781 Journal of Geophysical Research 118, 3744–3763.
782 Doval M., Castell N., Téllez L., and Mantilla E., 2012.The use of experimental data and their
783 uncertainty for assessing ozone photochemistry in the Eastern Iberian Peninsula.
784 Chemosphere, 89, 796-804.
785 EC, 2004. European Commission Decision of 19 March 2004 “Concerning guidance for
786 implementation of Directive 2002/3/EC of the European Parliament and the Council relating
787 to ozone in ambient air (2004/279/EC). Oficial Journal of the European Union L87/50 of
788 25.3.2004.
789 EEA, 2015. Air quality in Europe-2015 report. EEA Report, No 5/2015. ISSN 1977-8449.
790 Escudero M., Lozano A., Hierro J., del Valle J., and Mantilla E., 2014. Urban influence on increasing
791 ozone concentrations in a characteristic Mediterranean agglomeration. Atmospheric
792 Environment, 99, 322-332.
793 Gangoiti G., Millán M.M., Salvador R., and Mantilla E., 2001.Long-range transport and re-
794 circulation of pollutants in the western Mediterranean during the project Regional Cycles of
795 Air Pollution in the West-Central Mediterranean Area. Atmospheric Environment, 35, 6267-
796 6276.
797 Geiger R., Aron R.H. (1992). Todhunter P. The Climate Near the Ground. Rowman & Littelefield
798 Publishers Inc. 6th Edition.ISBN 0-7425-1857-4, Lonham, Us, 561 pp.
799 Gonçalves M., Jiménez-Guerrero P. and Baldasano J.M. 2009. Contribution of atmospheric
800 processes affecting the dynamics of air pollution in South-Western Europe during a typical
801 summertime photochemical episode. Atmos. Chem. Phys., 9, 849-864.
802 Hewson E.W. (1964). Industrial Air Pollution Meteorology. Meteorological Laboratories of the
803 College of Engineering. The University of Michigan. Ann Arbor, MI, 191 pp.
804 Kley D., Geiss H., 1994.Tropospheric ozone at elevated sites and precursor emissions in the United
805 States and Europe. Atmospheric Environment 8, 1, 149-158.

806 Lee, H.-K., Hwang, I.-K., Ahn, K.-H., 2014.Development and Evaluation of Hy-CPC. Particle and
807 Aerosol Research 10, 93-97.
808 Lee, H.-K., Eun, H.-R., Lee, G.-H., Ahn, K.-H., 2015.Development and evaluation of Hy-SMPS,
809 Particle and Aerosol Research 11, 57-61.
810 Mantilla E., Millán M.M., Sanz M.J., Salvador R., and Carratalá A., 1997. Influence of
811 mesometeorological processes on the evolution of ozone levels registered in the Valencian
812 Community. In: I Technical workshop on ozone pollution in southern Europe. Valencia.
813 Millán M.M. (Ed.), 2002. Ozone Dynamics in the Mediterranean Basin: A collection of scientific
814 papers resulting from the MECAPIP, RECAPMA and SECAP Projects. European Commission
815 (DG RTD I.2) Air Pollution Research Report 78, Available from CEAM, Valencia, Spain, 287 pp.
816 Millán, M.M. 2014. Extreme hydrometeorological events and climate change predictions in
817 Europe. J. Hydrol. 518B: 206-224.
818 Millán M.M., Artiñano B., Alonso L., Navazo M., Castro M., 1991. The effect of meso-scale flows on
819 regional and long-range atmospheric transport in the Western Mediterranean area.
820 Atmospheric Environment 25A, 5/6, 949-963.
821 Millán M.M., Salvador R., Mantilla E., Artiñano B., 1996a. Meteorology and photochemical air
822 pollution in southern Europe: experimental results from EC research projects. Atmospheric
823 Environment, 30, 1909-1924.
824 Millán M.M., Mantilla E., Salvador R., Kallos G., 1996b.Regional and long-range transport scenarios
825 for photo-oxidants on the Mediterranean basin in summer. Ninth joint conference on
826 applications of air pollution meteorology. 438-441. American Meteorological Society, Boston.
827 Millán M.M., Salvador R., Mantilla E., 1996c.Mesoscale processes and photo-oxidants cycles on the
828 Spanish Mediterranean coast. Ninth joint conference on applications of air pollution
829 meteorology.434-437. American Meteorological Society, Boston.
830 Millán M.M., Salvador R., Mantilla E., and Kallos G., 1997.Photooxidant dynamics in the
831 Mediterranean basin in summer: Results from European research projects. Journal of
832 Geophysical Research 102, 8811-8823.
833 Millán M.M. and Sanz M. J., 1999. Ozone in Mountainous regions and in Southern Europe. In: Ad
834 hoc Working group on Ozone Directive and Reduction Strategy Development, (eds.). Ozone
835 Position Paper.145-150. European Commission, Brussels.
836 Millán M.M., Mantilla E., Salvador R., Carratalá A., Sanz M.J., Alonso L., Gangoiti G., and Navazo
837 M., 2000. Ozone Cycles in the Western Mediterranean Basin: Interpretation of Monitoring
838 Data in Complex Coastal Terrain. Journal of Applied Meteorology, 39: 487-508.
839 Millán M.M., Sanz M.J., Salvador R., and Mantilla E., 2002. Atmospheric dynamics and ozone cycles
840 related to nitrogen deposition in the western Mediterranean. Environmental Pollution, 118,
841 167-186.
842 Minguillón M.C., Brines M., Pérez N., Reche C., Pandolfi M., Fonseca A.S., Amato F., Alastuey A.,
843 Lyasota A., Codina B., Lee H.-K., Eun H.-R., Ahn K.-H., Querol X., 2015. New particle formation
844 at ground level and in the vertical column over the Barcelona area. Atmospheric Research
845 164–165, 118–130.
846 Monks, P.S., Archibald A.T., Colette A., Cooper O., Coyle M., Derwent R., Fowler D., Granier C., Law
847 K.S., Mills G.E., Stevenson D.S., Tarasova O., Thouret V., von Schneidemesser E., Sommariva
848 R., Wild O., and Williams M.L., 2015. Tropospheric ozone and its precursors from the urban to
849 the global scale from air quality to short-lived climate forcer. Atmos. Chem. Phys., 15, 8889-
850 8973.
851 Palacios M., Kirchner F., Martilli A., Clappier A-. Martín F., Rodríguez M.E., 2002. Summer ozone
852 episodes in the Greater Madrid area. Analyzing the ozone response to abatement strategies
853 by modelling. Atmospheric Environment, 36, 5323–5333.

854 Pay, M.T., Valverde, V., Baldasano, J.M., Kwok, R., Napelenok, S., Baker, K., 2014.
855 PhotochemicalModeling to Attributing Source and Source Regions to Ozone Exceedances in
856 Spain. 13th Annual CMAS Conference, Chapel Hill, NC, October 27–29, 2014. Available at:
857 https://www.cmascenter.org/conference/2014/slides/maria_pay_photochemical_modeling_
858 2014.pptx.
859 Querol X., Alastuey A., Rodríguez S., Plana F., Ruiz C.R., Cots N., Massagué G., Puig O., 2001. PM10
860 and PM2.5 source apportionment in the Barcelona Metropolitan Area, Catalonia, Spain.
861 Atmospheric Environment 35/36, 6407-6419.
862 Querol X., Alastuey A., Orio A., Pallares M., Reina F., Dieguez JJ., Mantilla E., Escudero M., Alonso
863 L., Gangoiti G., Millán M. 2016. On the origin of the highest ozone episodes in Spain. Science
864 of the Total Environment, 572, 379-389.
865 Rodríguez S., Querol X., Alastuey A., Mantilla E., 2002. Origin of high summer PM10 and TSP
866 concentrations at rural sites in Eastern Spain. Atmospheric Environment 36, 3101-3112.
867 Salvador R., Millán M.M., and Calbo J., 1999.Horizontal Grid Size Selection and its influence on
868 Mesoscale Model Simulations. Journal of Applied Meteorology, 38, 1311-1329.
869 Salvador R., Millán M.M., Mantilla E., and Baldasano J.M., 1997.Mesoscale modelling of
870 atmospheric processes over the western Mediterranean area during summer. International
871 Journal of Environment and Pollution, 8, 513-528.
872 Seco, R., Peñuelas, J., Filella, I., Llusia, J., Schallhart, S., Metzger, A., Müller, M. and Hansel, A.,
873 2013. Volatile organic compounds in the western Mediterranean basin: urban and rural
874 winter measurements during the DAURE campaign. Atmos. Chem. Phys. 13, 8, 4291-4306.
875 Skamarock W.C., Klemp J.B., Gill D.O., Barker D.M. and J.G. Powers, 2008. A description of the
876 advanced research WRF version 3.NCAR. Tech. Note NCAR/TN-468+STR, 88pp. NCAR:
877 Boulder, Colorado, USA.
878 Soler, M.R.; Hinojosa, J., Bravo, M., Pino D., Vilà Guerau de Arellano, J., 2004. Analyzing the basic
879 features of different complex terrain flows by means a Doppler Sodar and a numerical model:
880 Some implications to air pollution problems. Meteorology and Atmospheric Physics, 1-3,
881 141,154.
882 Soler M.R., Arasa, A., Merino M., Olid M. and Ortega S., 2011.High vertical resolution numerical
883 simulation of the sea-breeze flow in Catalonia. Implications to spatial and temporal variability
884 of ozone and PM10 levels. Bound.-Layer Meteor, 140, 37-56.
885 Soler R.M., Gámez P. and Olid M., 2015. Aramis a regional air quality model for air pollution
886 management: evaluation and validation. Física de la Tierra, 27, 111-136
887 Stein A.F., Mantilla E., and Millán M.M., 2004.Ozone formation downwind an industrial complex in
888 the western Mediterranean. In: 13th World Clean Air and Environmental Protection. August
889 22-27. London, U.K.
890 Stein A.F., Mantilla E., and Millán M.M., 2005. Using measured and modelled indicators to assess
891 ozone-NOx-VOC sensitivity in a western Mediterranean coastal environment. Atmospheric
892 Environment, 39: 7167-7180.
893 Tang Y.S., Cape J.N., Sutton M.A., 2001. Development and types of passive samplers for NH_3 and
894 NOx. In: Proceedings of the International Symposium on Passive Sampling of Gaseous
895 Pollutants in Ecological Research. Science World, vol. 1, pp. 513-529.
896 Toll, I., Baldasano, J.M., 2000.Modeling of photochemical air pollution in the Barcelona area with
897 highly disaggregated anthropogenic and biogenic emissions. Atmos. Environ.34, 3069–3084.
898 UNECE, 2010.Hemispheric transport of air pollution 2010. Part A: ozone and particulate matter. Air
899 pollution studies, 17. UNECE, LRTAP, Task Force on Hemispheric Transport of Pollutants HTAP
900 2010: Part A. Ozone and Particulate Matter, 278 pp, ECE/EB.AIR/100, ISBN 978-92-1-117043-6

Atmos. Chem. Phys. Discuss., doi:10.5194/acp-2016-925, 2016
Manuscript under review for journal Atmos. Chem. Phys.
Published: 10 November 2016

Atmospheric Chemistry and Physics Discussions

http://www.htap.org/publications/2010_report/2010_Final_Report/HTAP%202010%20Part%20A%20110407.pdf

Valverde V., Pay M.T., Baldasano J.M., 2016. Ozone attributed to Madrid and Barcelona on-road transport emissions: Characterization of plume dynamics over the Iberian Peninsula. Science of the Total Environment 543, 670–682.

Atmos. Chem. Phys. Discuss., doi:10.5194/acp-2016-925, 2016
Manuscript under review for journal Atmos. Chem. Phys.
Published: 10 November 2016

Atmospheric Chemistry and Physics Discussions

907 **FIGURE AND TABLE CAPTIONS**

908 Figure 1. Top: Study area and location of monitoring sites (regional air quality monitoring sites
909 XVPCA, dosimeters, meteorological stations and vertical measurements). BMA: Barcelona
910 Metropolitan Area. Bottom: Topographic profiles across the study area, red arrows point to the
911 valleys connecting BMA with the Bic Plain and the Pre-Pyrenean regions.

912 Figure 2. Mean hourly (UTC) values for meteorological parameters and gaseous and particulate
913 pollutants for 03-06, 14-20 and 10-17/7/2015 recorded at VIC with the laboratory van (10-
914 17/07/2015), with the exception of O_3, measured at the same location but by the permanent VIC
915 XVPCA station, and the meteorological data obtained from Gurb station (Meteocat) located 1 km
916 to the north of VIC.

917 Figure 3. O_3 hourly concentrations recorded at the coastal (BEG, blue) and remote inland western
918 pre-Pyrenean (MSC, clear green, 1570 m a.s.l.) sites, 2 urban background sites of Barcelona (PLR,
919 CTL, grey and black), 2 urban sites in the northern periphery of the Barcelona's metropolitan area
920 (GRA, MON, orange and yellow), the inner Vic Plain sites (TON, VIC and MAN, red, pink and violet)
921 and the remote eastern pre-Pyrenean site of PAR (brown), along July 2015.

922 Figure 4. Polar plots of hourly O_3 concentrations in the real-time measurement sites.

923 Figure 5. O_3 and O_X (O_3+NO_2) hourly concentrations recorded at the coastal (BEG, blue, at this site
924 only O_3 is available because the lack of NO_2 measurements), an urban background site of
925 Barcelona (CTL, black), an urban site in the northern periphery of the Barcelona's metropolitan
926 area (GRA, orange), the intermediate inland rural site of MSY (720 m a.s.l., green), and the inner
927 Vic Plain site (TON, red) along July 2015. The pink and blue squares mark the A and B O_3 and O_X
928 episodes distinguished in this study, respectively.

929 Figure 6. Mean hourly levels of O_3 and O_X (O_3+NO_2) for sites located in a south and coast to north-
930 inland (CTL, GRA and BEG, and MSY, TON, VOIC, MAN and PAR, respectively) following the inland
931 transport of pollutants and maxima time shift according to this breeze transport (right) for the
932 periods 3-6/07/2015 (B type episode, left) and 14-20/07/2015 (A type episode, right). Time is UTC.

933 Figure 7. Top: Hourly O_3 maxima (and number of hours exceeding 180 µg/m^3) in the study sites
934 with real time O_3 measurements (shadowed areas indicate 2 different degrees of exceedances, 1-3
935 h and 13-23h). Bottom: Frequency of occurrence of hourly (UTC) O_3 exceedances of 180 µg/m^3
936 along the day; both for July 2015.

937 Figure 8. Vertical profiles of particle number concentrations for particles >3 nm (red, N_3), 0.3-0.5
938 µm (blue, $PM_{0.3-0.5}$), 0.5-1.0 µm ($PM_{0.5-1}$) and wind direction obtained with the tethered balloon
939 measurements on 14 and 17/07/2015.

940 Figure 9. Vertical profiles of O_3, temperature and relative humidity obtained with the tethered
941 balloon measurements on 14 and 17/07/2015.

Atmos. Chem. Phys. Discuss., doi:10.5194/acp-2016-925, 2016
Manuscript under review for journal Atmos. Chem. Phys.
Published: 10 November 2016

Atmospheric Chemistry and Physics Discussions

942 Figure 10.Time variation of altitude, temperature, relative humidity, N_3, particle number size
943 distributions and O_3 concentrations during the tethered balloon measurements on 16/07/2015. 1
944 to 3 illustrate the nucleation episode recorded at surface level with particle number size
945 distributions, and 4 the typical regional background size N size distribution at around 300 m over
946 the ground.

947 Figure 11. Vertical profiles of BC (5 min time resolution) and O_3 (10 seconds time resolution) at
948 VIC.

949 Figure 12. Mean hourly O_3 concentrations, and wind speed and wind direction for the episodes A
950 and B, showing higher levels in the A episodes for the two O_3 maxima.

951 Figure 13. Maps of simulated NO_2 and O_3 concentrations at ground level and 1000m a.g.l., and
952 horizontal wind fields at 10 m a.g.l. for selected hours on 03/07/2015.

953 Figure 14. Maps of simulated NO_2 and O_3 concentrations at ground level and 1000m a.g.l., and
954 horizontal wind fields at 10 m a.g.l. for selected hours on 15/07/2015.

955 Figure 15. Spatial distributions of simulated O_3 concentrations and wind field vectors in the south–
956 north vertical cross-section for different hours on 03 and 15/07/2015.

957

958

Atmos. Chem. Phys. Discuss., doi:10.5194/acp-2016-925, 2016
Manuscript under review for journal Atmos. Chem. Phys.
Published: 10 November 2016

Atmospheric Chemistry and Physics Discussions

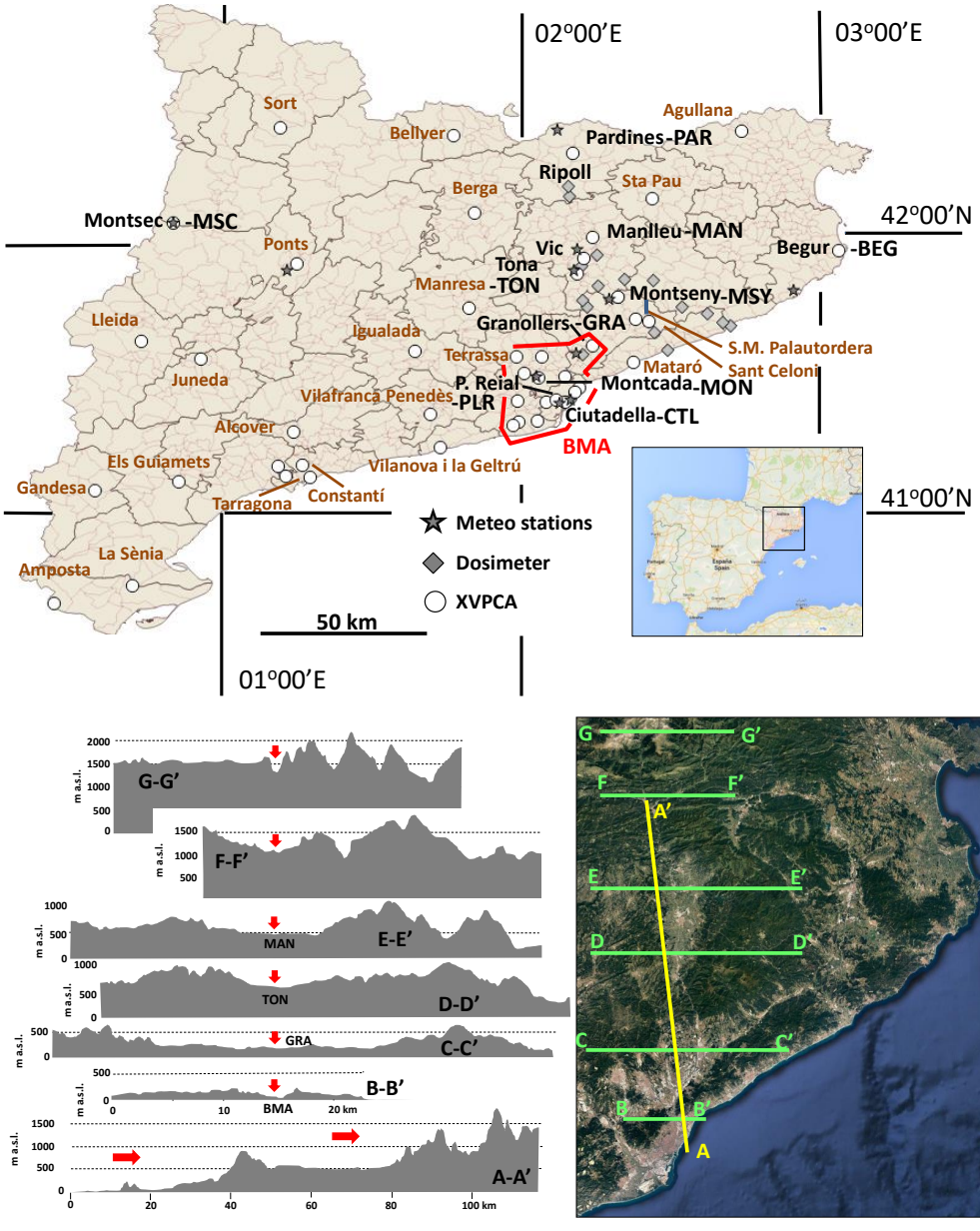

959

960
961

962 Figure 1

Atmos. Chem. Phys. Discuss., doi:10.5194/acp-2016-925, 2016
Manuscript under review for journal Atmos. Chem. Phys.
Published: 10 November 2016

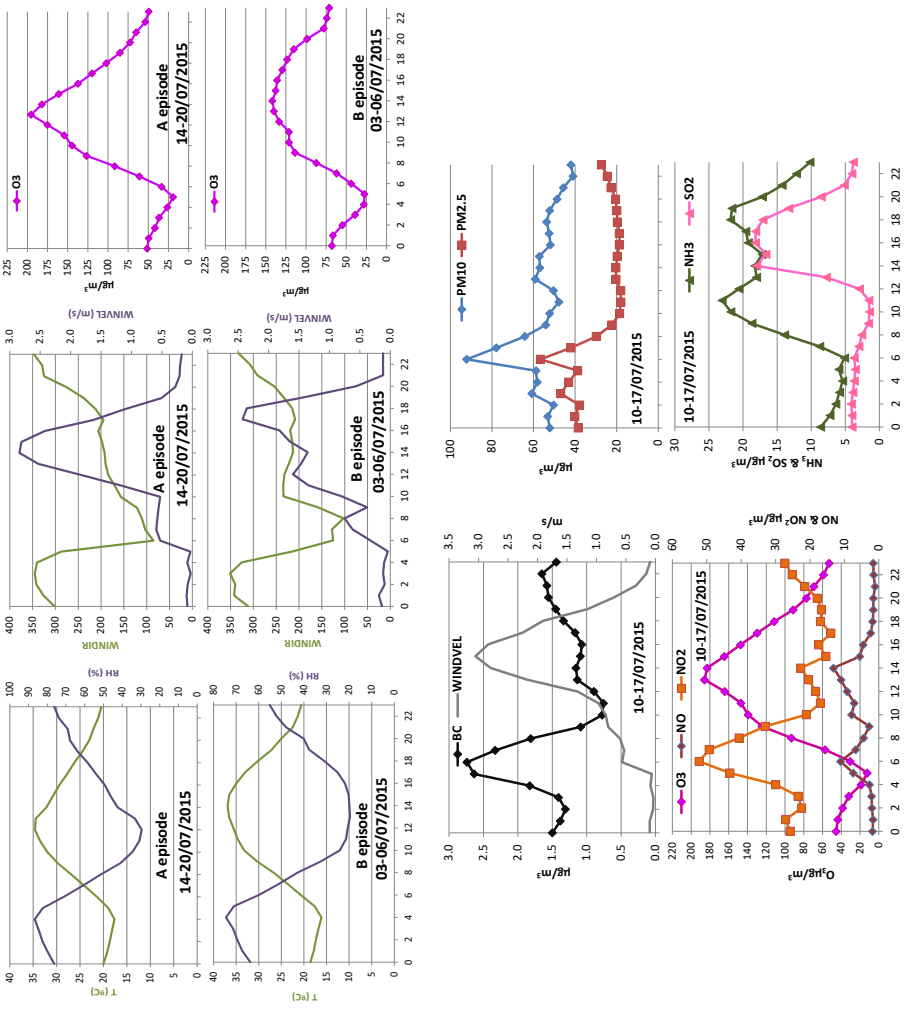

Figure 2

Atmos. Chem. Phys. Discuss., doi:10.5194/acp-2016-925, 2016
Manuscript under review for journal Atmos. Chem. Phys.
Published: 10 November 2016

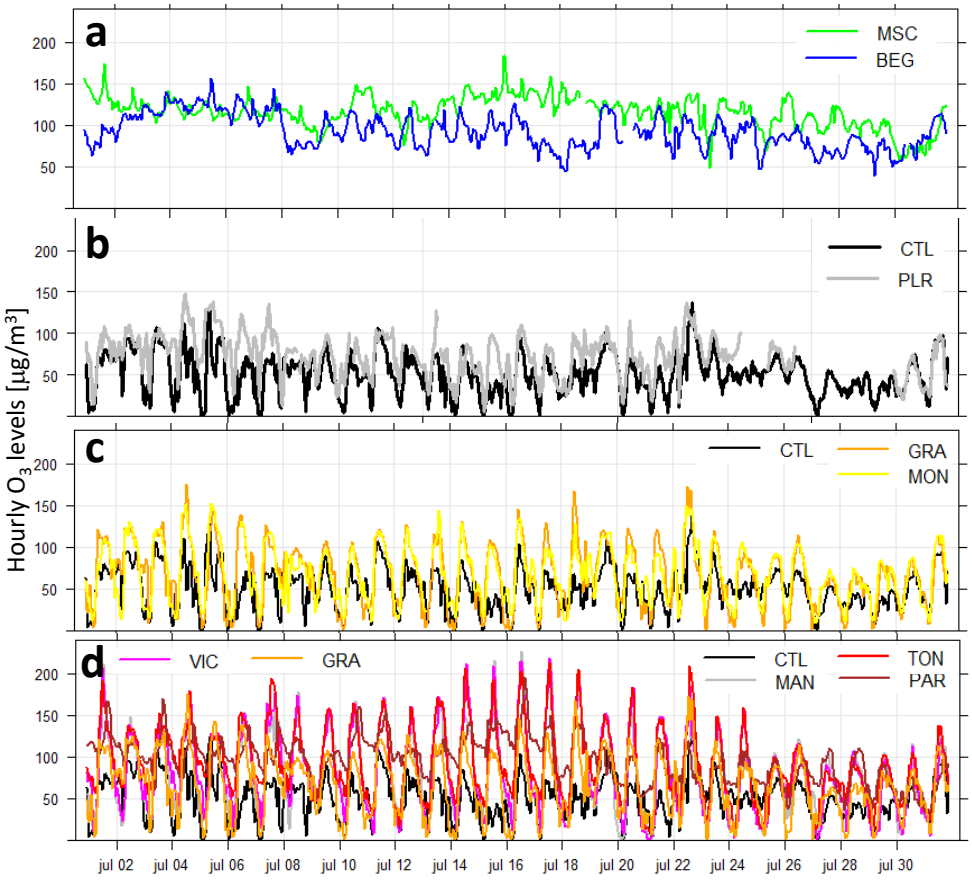

FIGURE 3

Atmos. Chem. Phys. Discuss., doi:10.5194/acp-2016-925, 2016
Manuscript under review for journal Atmos. Chem. Phys.
Published: 10 November 2016

Atmospheric Chemistry and Physics Discussions
Open Access
EGU

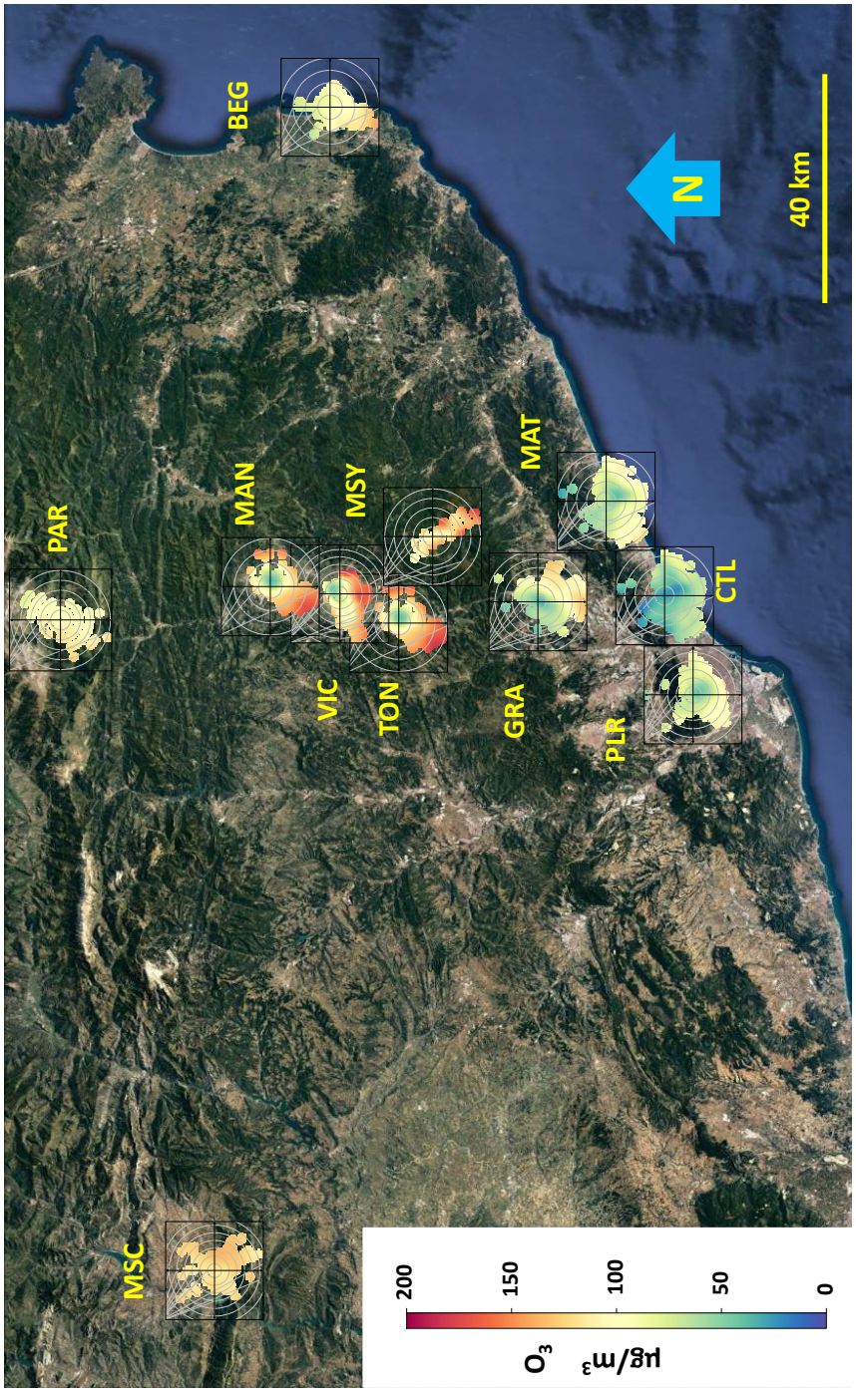

FIGURE 4

Atmos. Chem. Phys. Discuss., doi:10.5194/acp-2016-925, 2016
Manuscript under review for journal Atmos. Chem. Phys.
Published: 10 November 2016

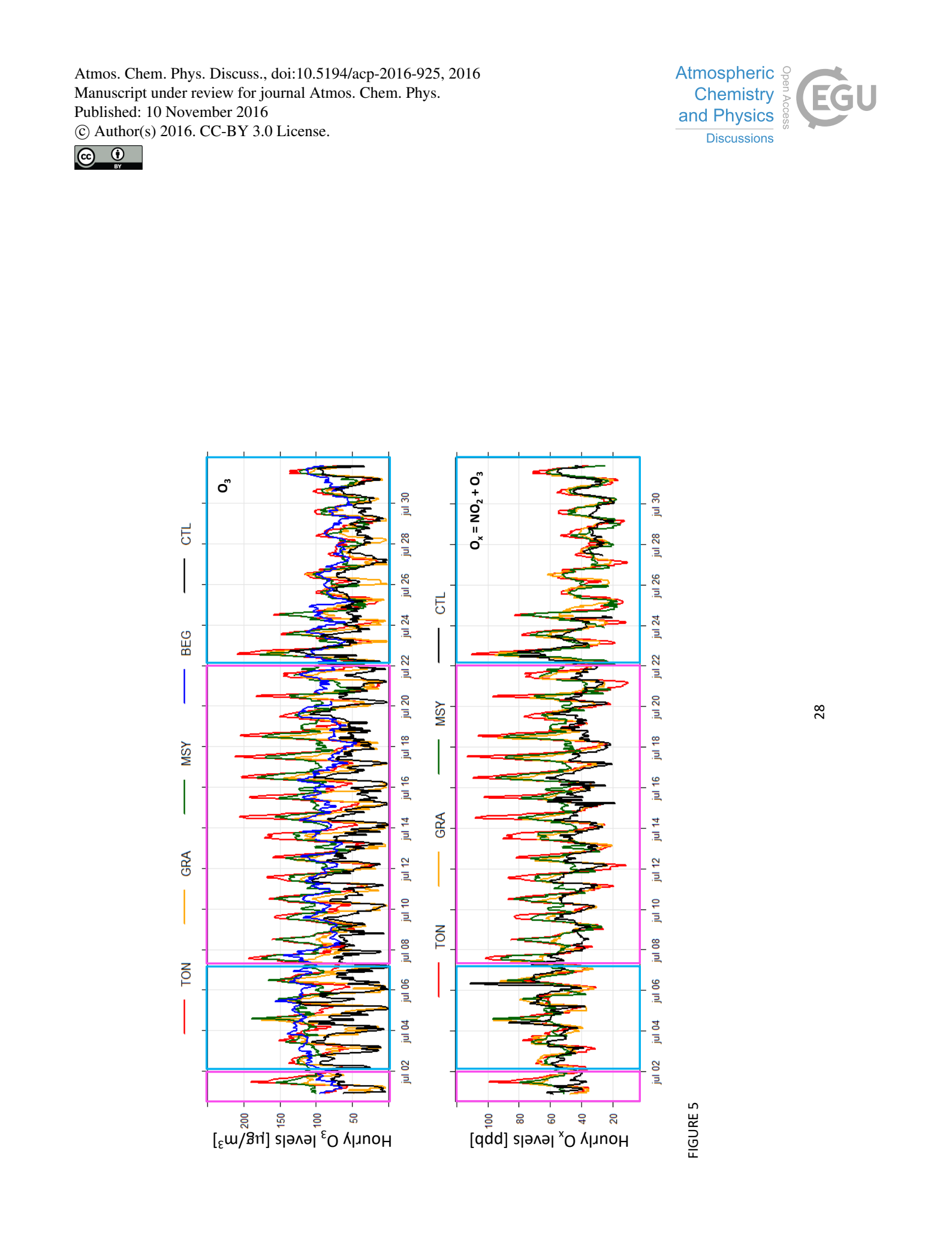

FIGURE 5

Atmos. Chem. Phys. Discuss., doi:10.5194/acp-2016-925, 2016
Manuscript under review for journal Atmos. Chem. Phys.
Published: 10 November 2016

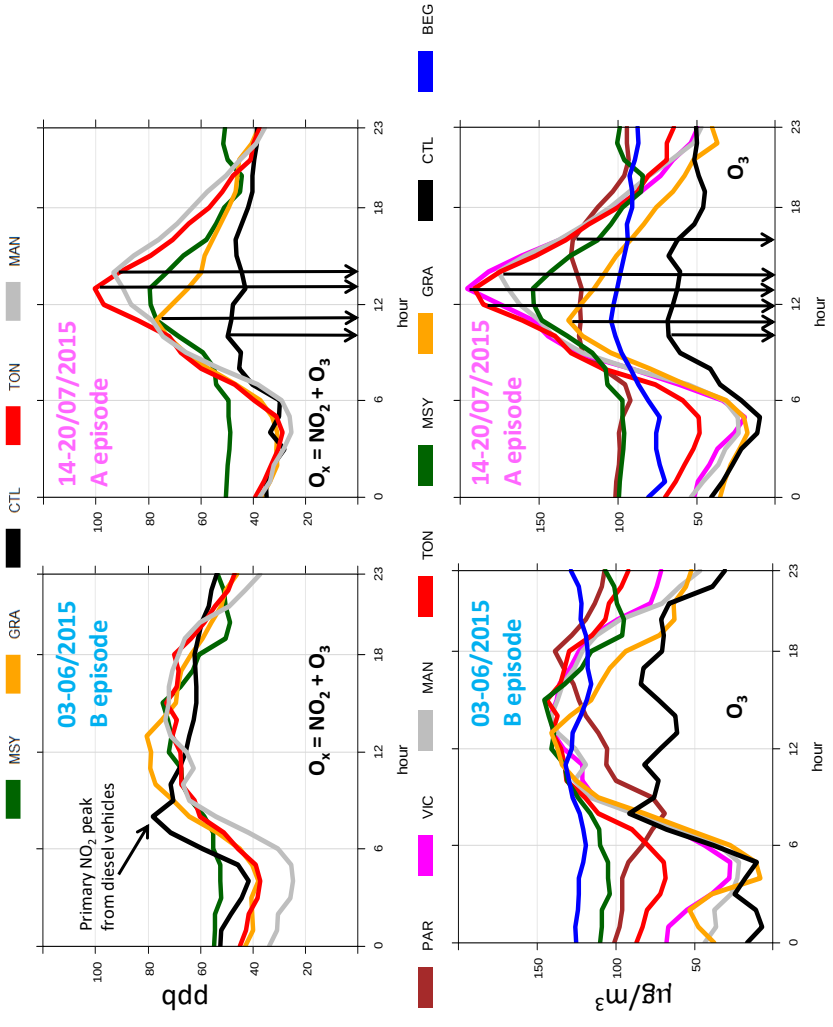

FIGURE 6.

Atmos. Chem. Phys. Discuss., doi:10.5194/acp-2016-925, 2016
Manuscript under review for journal Atmos. Chem. Phys.
Published: 10 November 2016

Atmospheric Chemistry and Physics Discussions

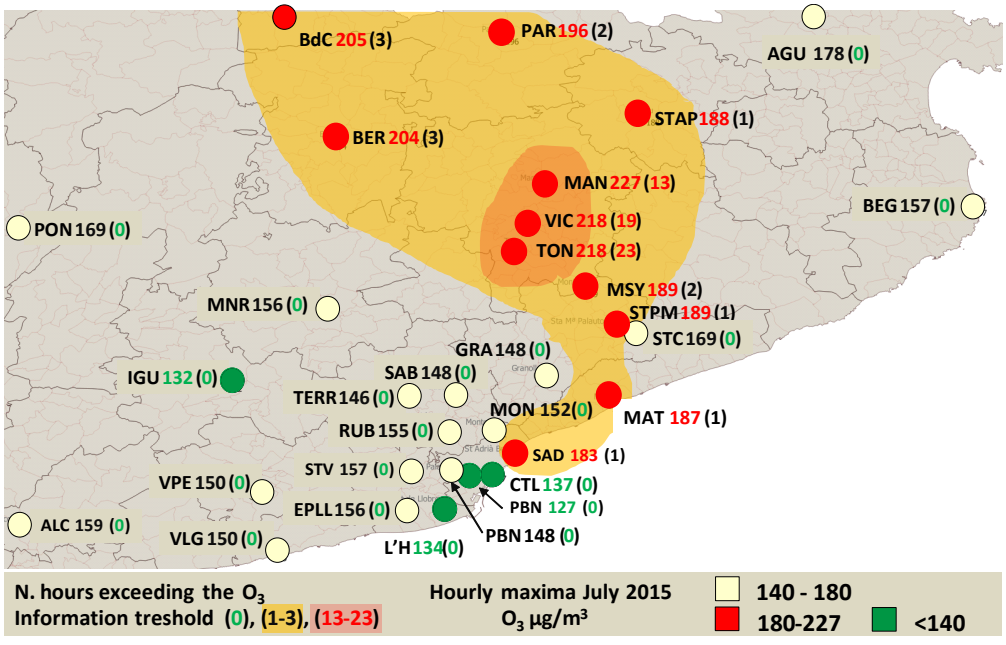

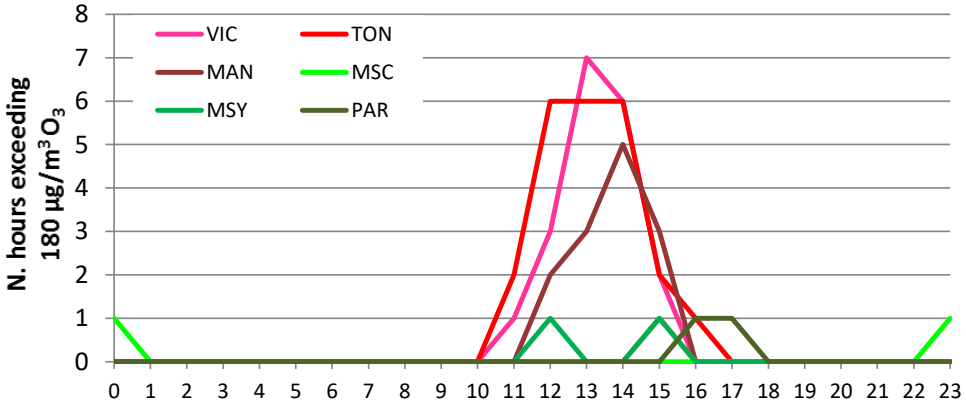

FIGURE 7.

Atmos. Chem. Phys. Discuss., doi:10.5194/acp-2016-925, 2016
Manuscript under review for journal Atmos. Chem. Phys.
Published: 10 November 2016

Atmospheric Chemistry and Physics Discussions

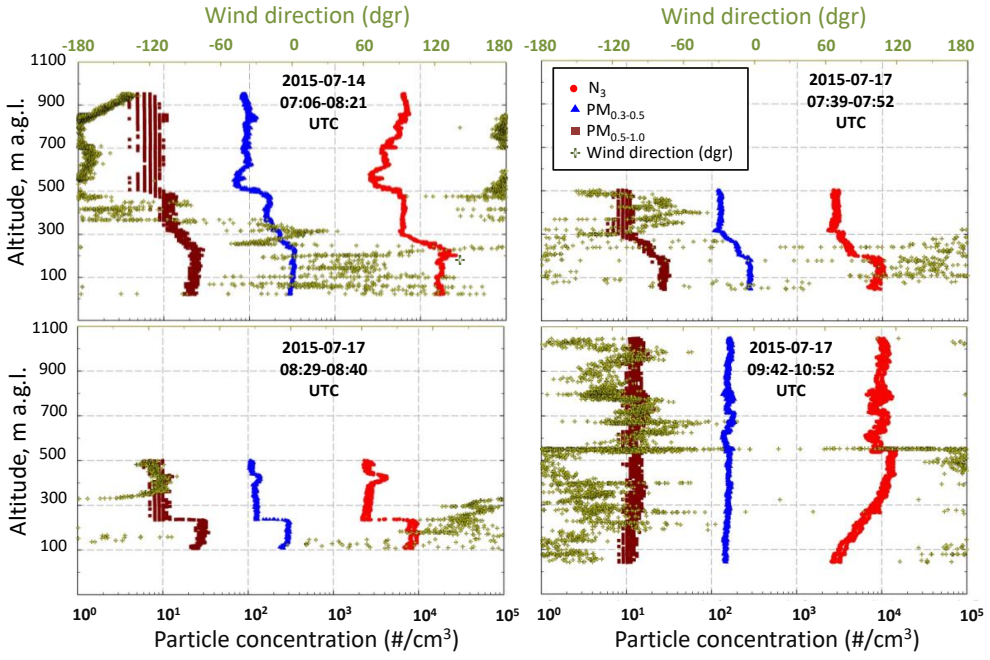

FIGURE 8.

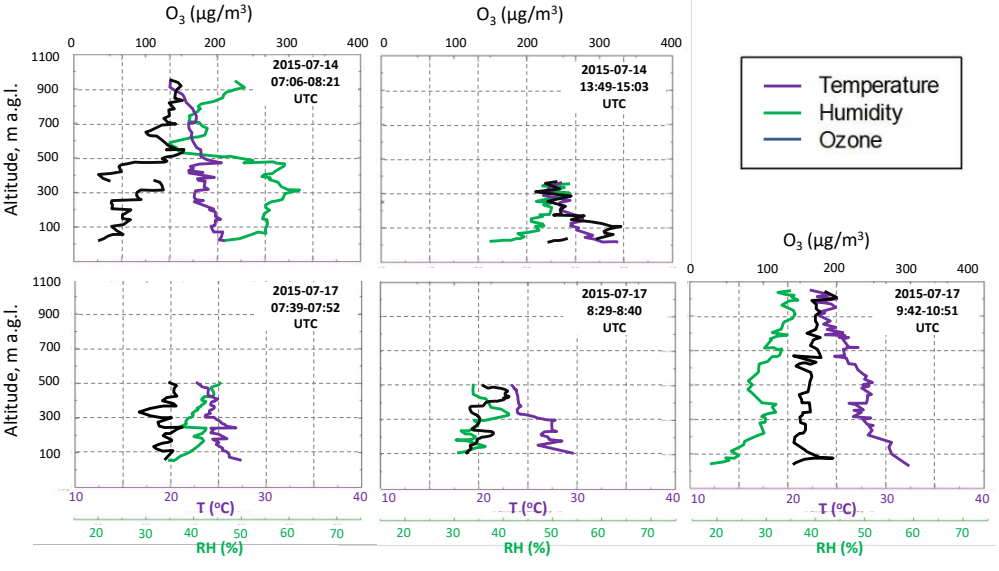

FIGURE 9

Atmos. Chem. Phys. Discuss., doi:10.5194/acp-2016-925, 2016
Manuscript under review for journal Atmos. Chem. Phys.
Published: 10 November 2016

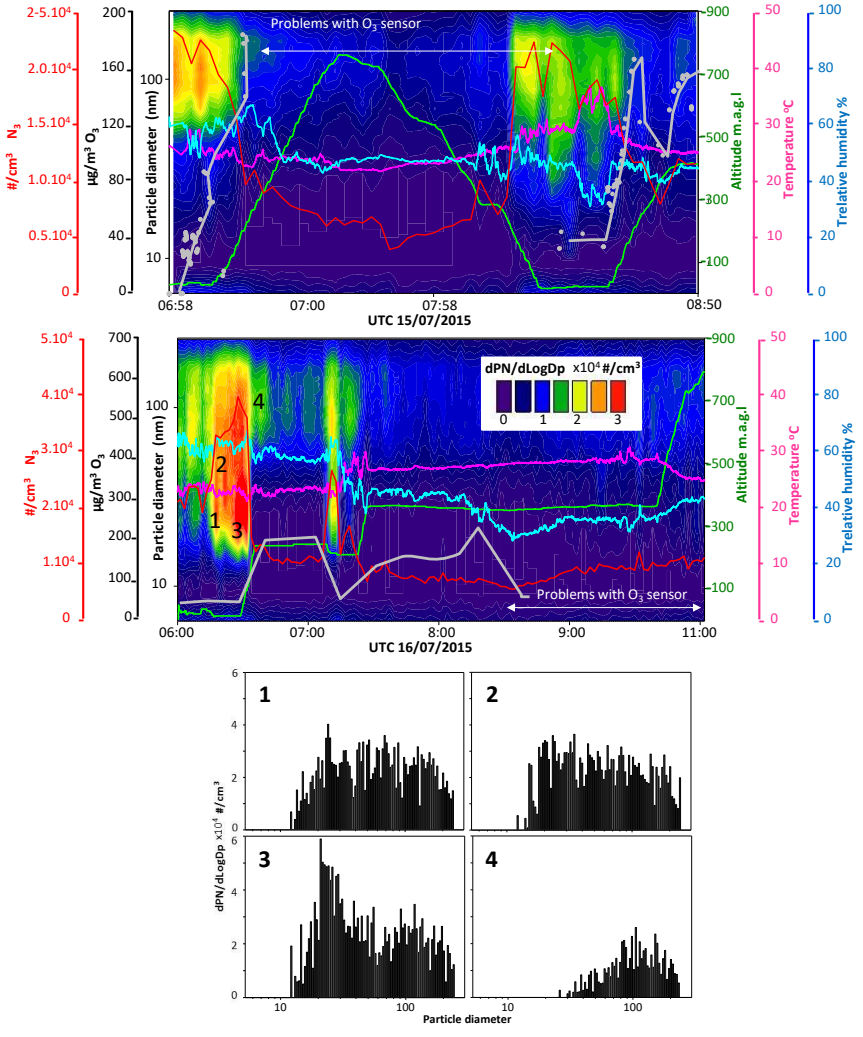

FIGURE 10

Atmos. Chem. Phys. Discuss., doi:10.5194/acp-2016-925, 2016
Manuscript under review for journal Atmos. Chem. Phys.
Published: 10 November 2016

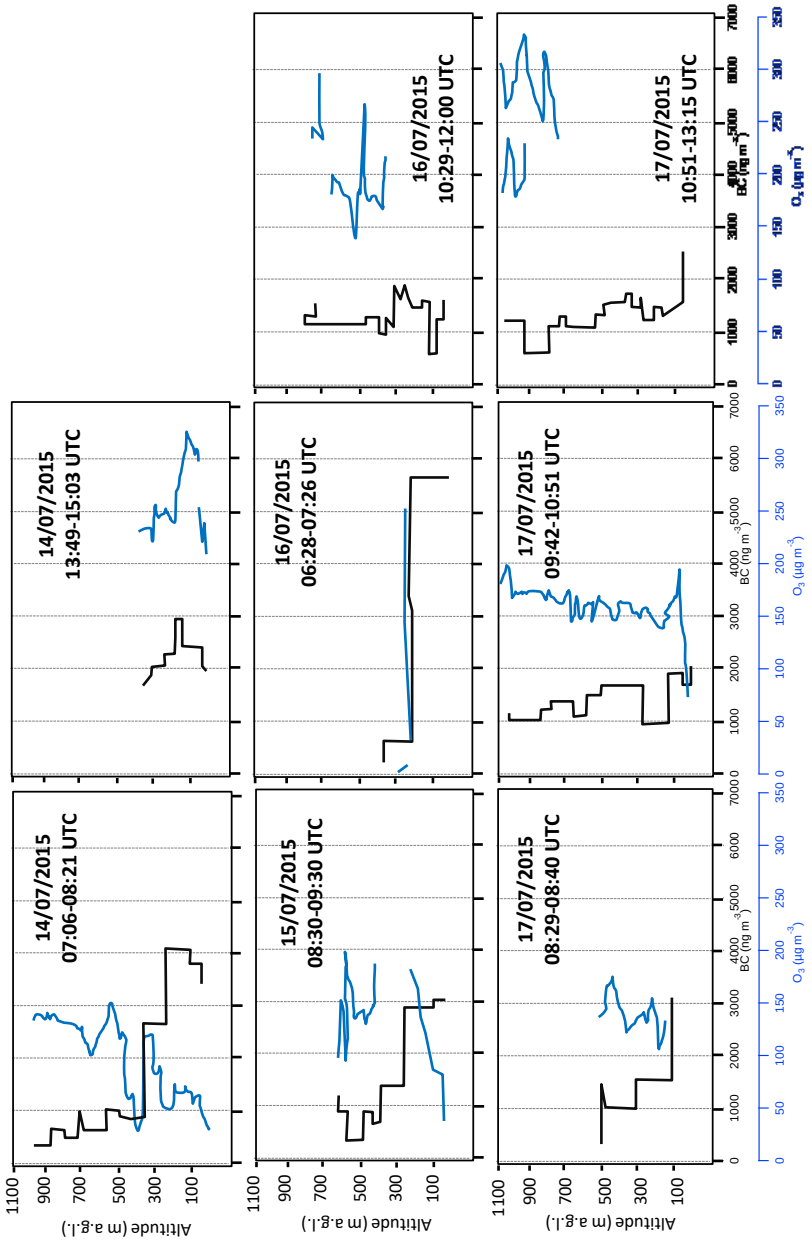

FIGURE 11

Atmos. Chem. Phys. Discuss., doi:10.5194/acp-2016-925, 2016
Manuscript under review for journal Atmos. Chem. Phys.
Published: 10 November 2016

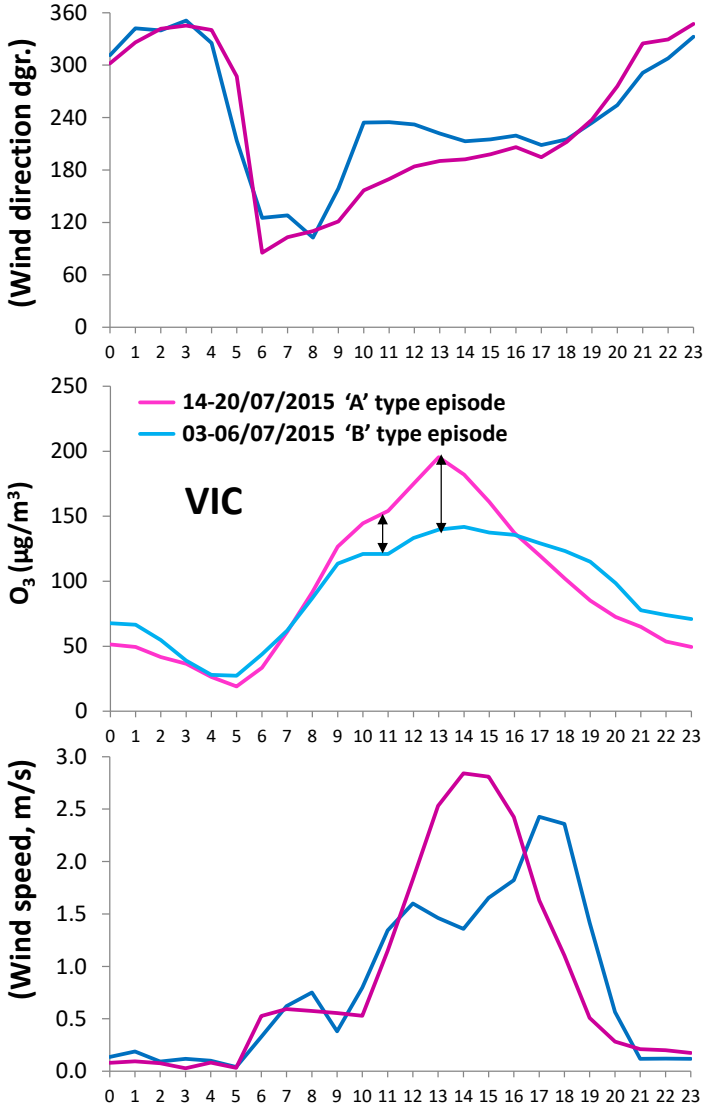

FIGURE 12

Atmos. Chem. Phys. Discuss., doi:10.5194/acp-2016-925, 2016
Manuscript under review for journal Atmos. Chem. Phys.
Published: 10 November 2016

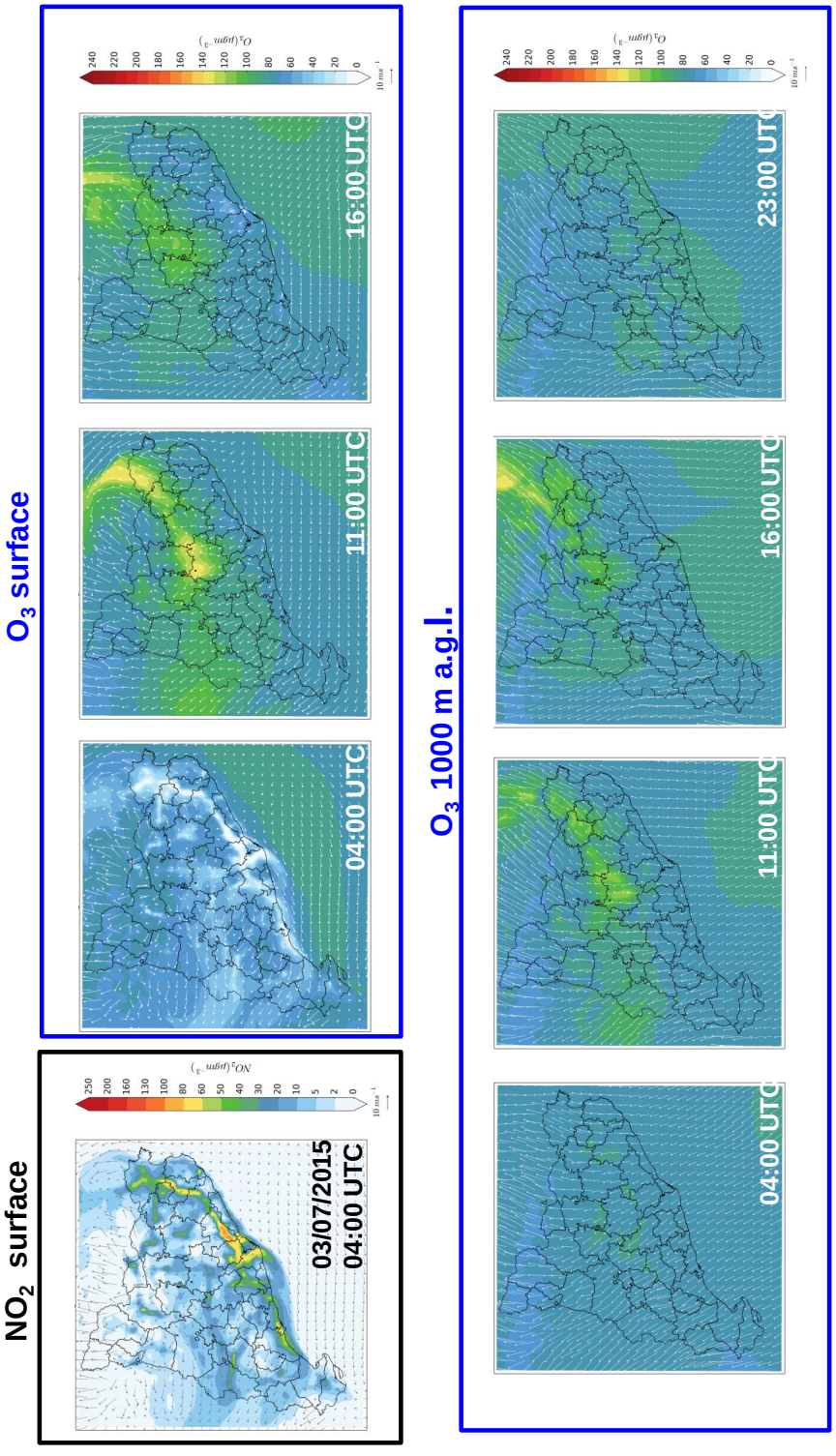

FIGURE 13

Atmos. Chem. Phys. Discuss., doi:10.5194/acp-2016-925, 2016
Manuscript under review for journal Atmos. Chem. Phys.
Published: 10 November 2016

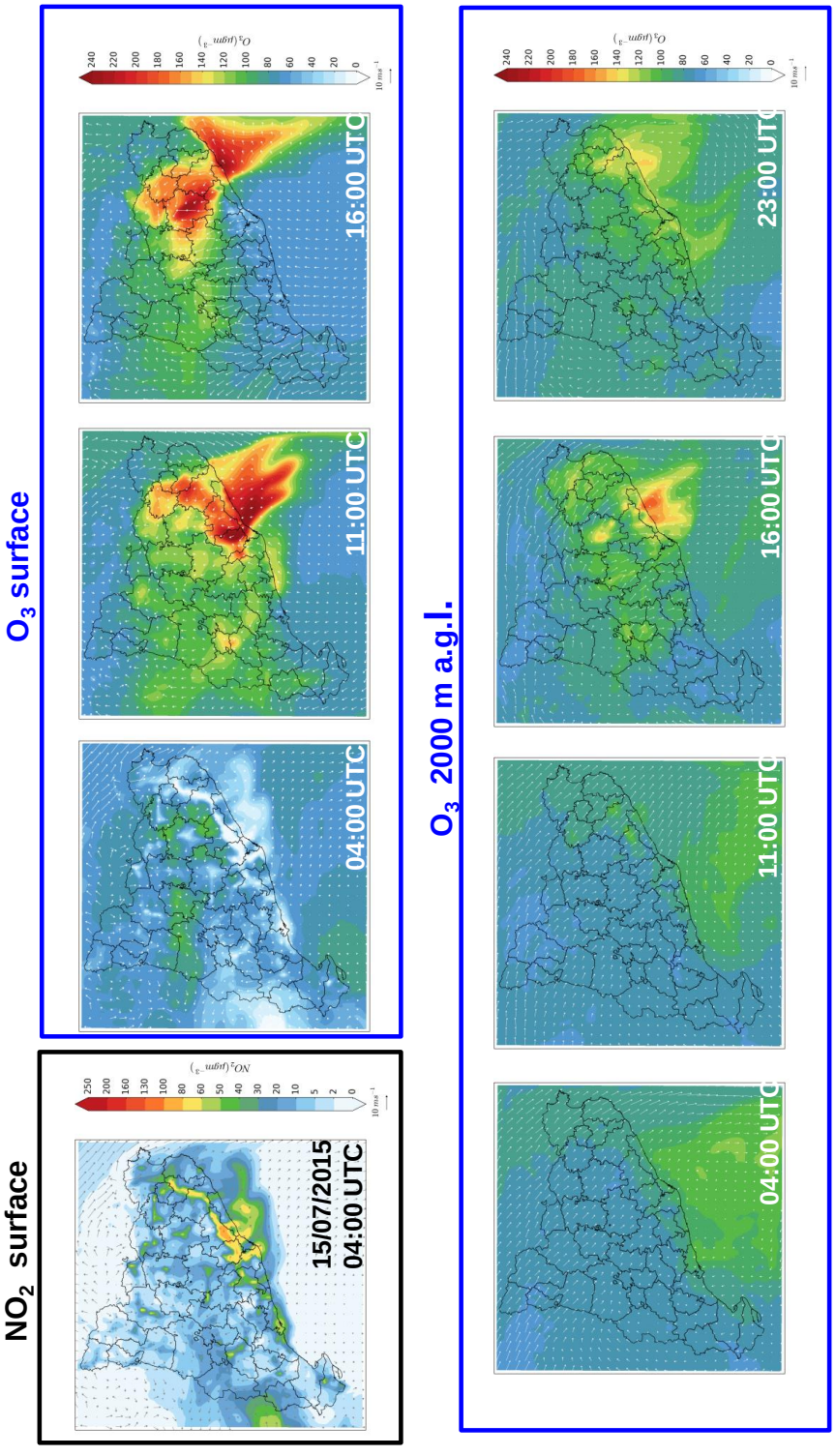

FIGURE 14

Atmos. Chem. Phys. Discuss., doi:10.5194/acp-2016-925, 2016
Manuscript under review for journal Atmos. Chem. Phys.
Published: 10 November 2016

Atmospheric Chemistry and Physics Discussions

FIGURE 15